SLAC Summer Institute 2016

"New Horizons on the Energy Frontier"

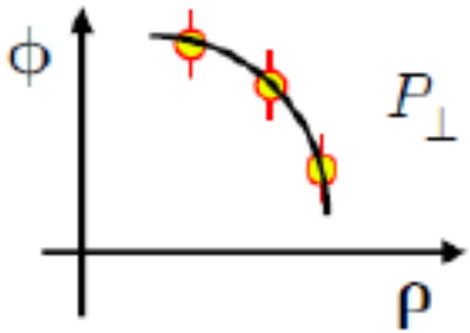

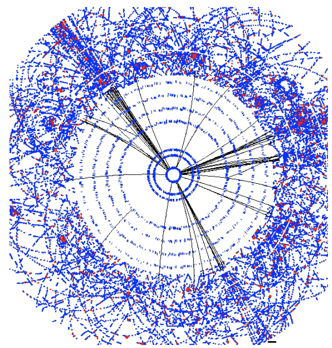

Tracking Detectors (Lecture 1)

Norbert Wermes
University of Bonn

Outline

Lecture 1

- ❑ Requirements on tracking detectors
- ❑ Gas/semiconductor detectors in comparison
- ❑ How the signal develops
  - Shockley-Ramo theorem
  - Weighting fields in various configurations
- ❑ Diffusion and drift (short)
- ❑ Space resolution w/ patterned electrodes
- ❑ Gas-filled detectors
  - Gas amplification (streamers and sparks)
  - The drift chamber
  - The "Time Projection" chamber
  - What is different at LHC experiments?

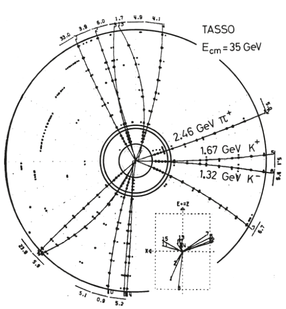

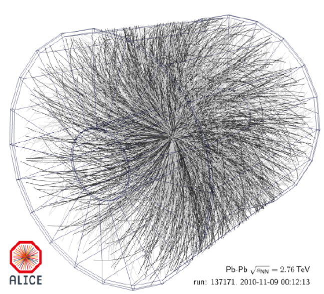

Lecture 2

- ❑ How to make a semiconductor detector?
- ❑ The nuisance of δ-electrons
- ❑ Radiation damage: NIEL and IEL (TID)
- ❑ What to do for High-Lumi LHC?
- ❑ Alternatives to "Hybrid" Pixels
  - DEPFET Pixels
  - DMAPS: Monolithic CMOS Pixels
- ❑ 4D with LGADs?

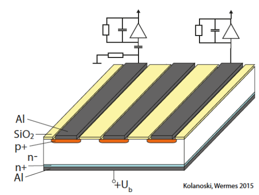

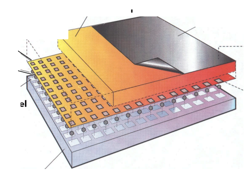

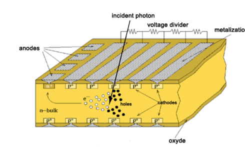

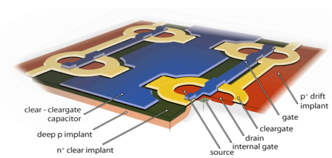

Tasks of Tracking detectors

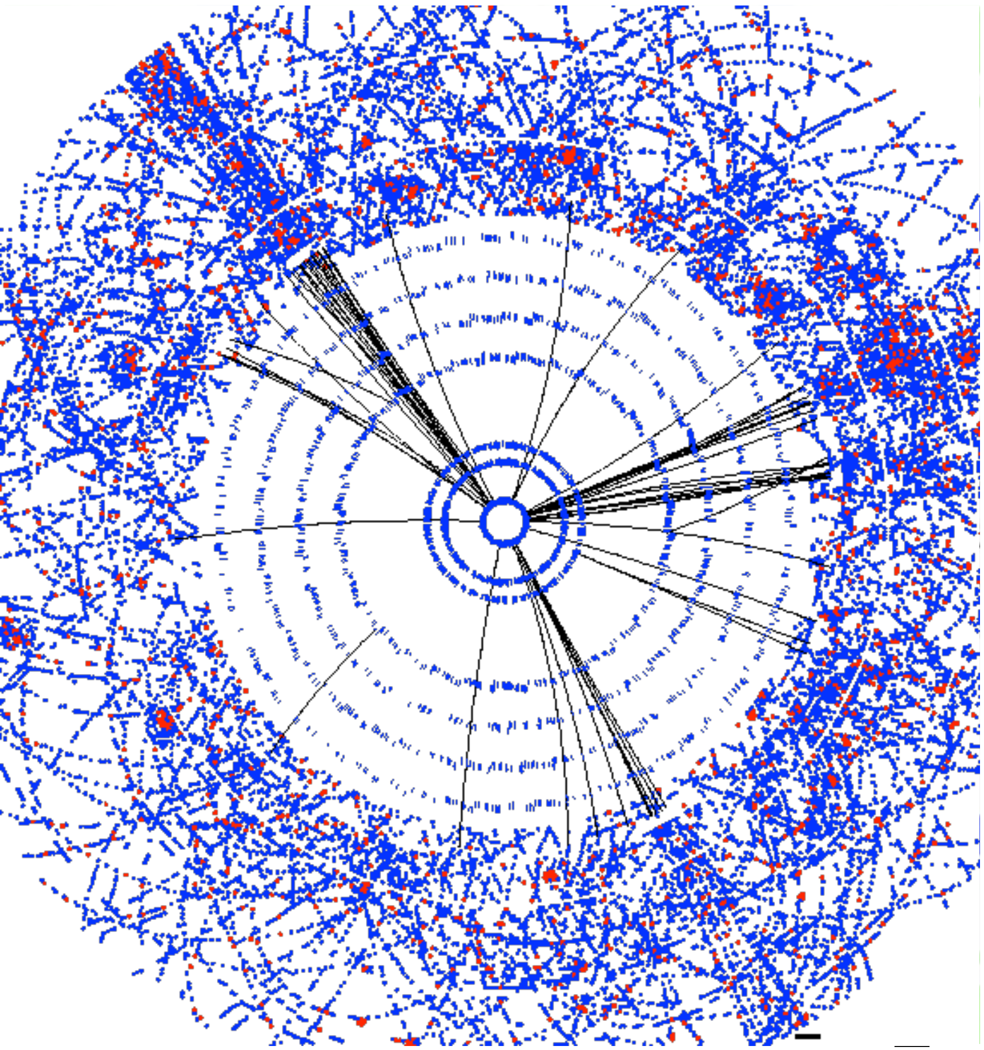

$H \to b\bar{b}$

- provide precise space points or space point clusters (vectors) originating from ionizing charged particles

  allowing
  - particle track finding from patterns of measured hits (at large background & pile-up)
  - momentum (B-field) and angle measurement
  - measurement of primary and secondary vertices
  - multi-track separation and vertex-ID in the core of (boosted) jets
  - measurement of specific ionization for low momentum tracks (not this talk)

- keep the material influencing the paths of particles to a minimum to avoid scattering and secondary interactions

see also lecture by Christian Weiser

Track models

- In a homogeneous B-field the motion of a charged particle is a helix.
- The projection can be parametrized by a linearized circle

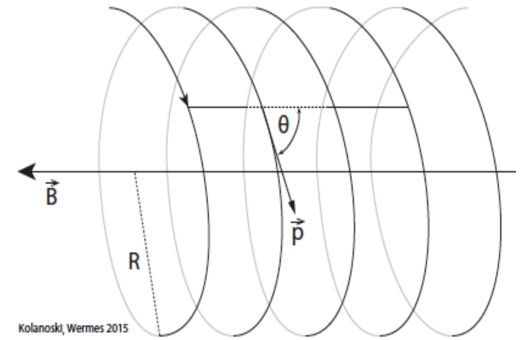

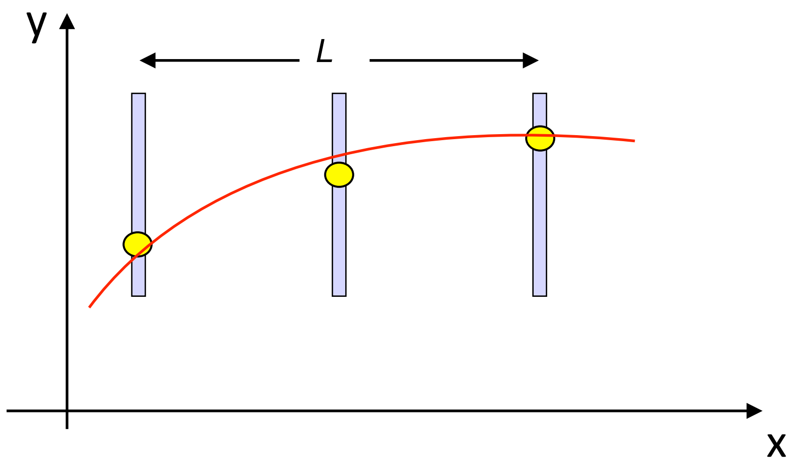

$$y = y_0 + \sqrt{R^2 - (x - x_0)^2}$$

$$\Rightarrow y \approx a + bx + \frac{1}{2}cx^2$$

- This track model is fit (χ^2) to measured space points

$$S = \sum_{i=1}^{N}\sum_{j=1}^{N}(\xi_i^{meas} - \xi_i^{fit})\, V_{y,ij}^{-1}\, (\xi_j^{meas} - \xi_j^{fit}) \quad = \sum_{i=1}^{N}\frac{(\xi_i^{\mathrm{mess}} - \xi_i^{fit}(\theta))^2}{\sigma_i^2}$$

if V is diagonal

Track models

$$\Rightarrow y \approx a + bx + \frac{1}{2}cx^2$$

- yielding the parameters a, b, and c and their errors
  - here N equidistant measurements

$$\sigma_a^2 = \sigma^2 \frac{3N^2-7}{4(N-2)N(N+2)}$$

$$\sigma_b^2 = \frac{\sigma^2}{L^2}\frac{12(N-1)}{N(N+1)}$$ slope

$$\sigma_c^2 = \frac{\sigma^2}{L^4}\frac{720(N-1)^3}{(N-2)N(N+1)(N+2)}$$ curvature

$$\sigma_{ab} = \sigma_{bc} = 0$$

$$\sigma_{ac} = \frac{\sigma^2}{L^2}\frac{30N}{(N-2)(N+2)}$$

- ... and the errors on the track coordinates y at a given x

$$\sigma_y^2 = \sum_{i=1}^{m}\sum_{j=1}^{m}\frac{\partial y}{\partial \theta_i}\frac{\partial y}{\partial \theta_j}V_{\theta,ij}$$

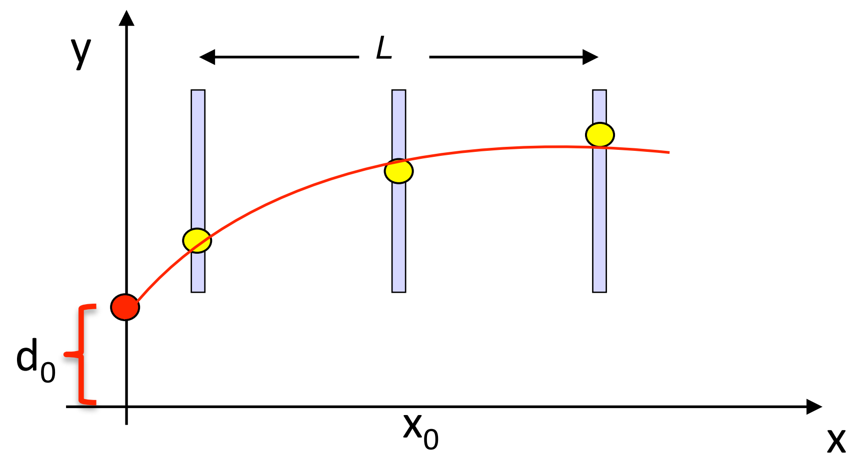

e.g. : the impact parameter resolution

$$\sigma_y = \sigma_{d_0} = \sqrt{\sigma_a^2 + x_0^2\,\sigma_b^2 + \frac{1}{4}x_0^4\,\sigma_c^2 + x_0^2\,\sigma_{ac}}$$

$$= \frac{\sigma_{meas}}{\sqrt{N}}\sqrt{1 + r^2\frac{12(N-1)}{(N+1)} + r^4\frac{180(N-1)^3}{(N-2)(N+1)(N+2)} + r^2\frac{30N^2}{(N-2)(N+2)}}$$

$r = x_0/L$
= extrapolation parameter

Track models

For N equidistant points we get for the curvature:

for N > 10

$$\sigma_c = \frac{\sigma_{\text{meas}}}{L^2}\sqrt{\frac{720(N-1)^3}{(N-2)N(N+1)(N+2)}} \approx \frac{\sigma_{\text{meas}}}{L^2}\sqrt{\frac{720(N-1)}{(N+4)}}$$

and for the transverse momentum

$$p_T = |q|\,B\,R = \frac{q\,B}{\kappa}$$

$$\left(\frac{\sigma_{p_T}}{p_T}\right)_{\text{meas}} = \frac{p_T}{0.3|z|}\frac{\sigma_{\text{meas}}}{L^2 B}\sqrt{\frac{720}{N+4}}$$

$$[p_T] = \text{GeV/c},\ [L] = \text{m},\ [B] = \text{T}$$

Gluckstern formula

NIM 24 (1963) 381

material contributes
via multiple scattering

$$\left(\frac{\sigma_{p_T}}{p_T}\right)_{\text{MS}} = \frac{0.054}{L\,B\,\beta}\sqrt{\frac{L/\sin\theta}{X_0}}$$

Total momentum resolution

$$\frac{\sigma_{p_T}}{p_T} = \sqrt{\left(\frac{\sigma_{p_T}}{p_T}\right)^2_{\text{meas}} + \left(\frac{\sigma_{p_T}}{p_T}\right)^2_{\text{MS}}}$$

example: LEP detector OPAL

L = 1.6 m, B = 35 T, N = 159, σ_{mess}= 135 µm

$$\frac{\sigma_{p_T}}{p_T} = \sqrt{(0.15\% p_T)^2 + (2\%)^2}$$

= 2% @ 1 GeV

= 7.5% @ 50 GeV

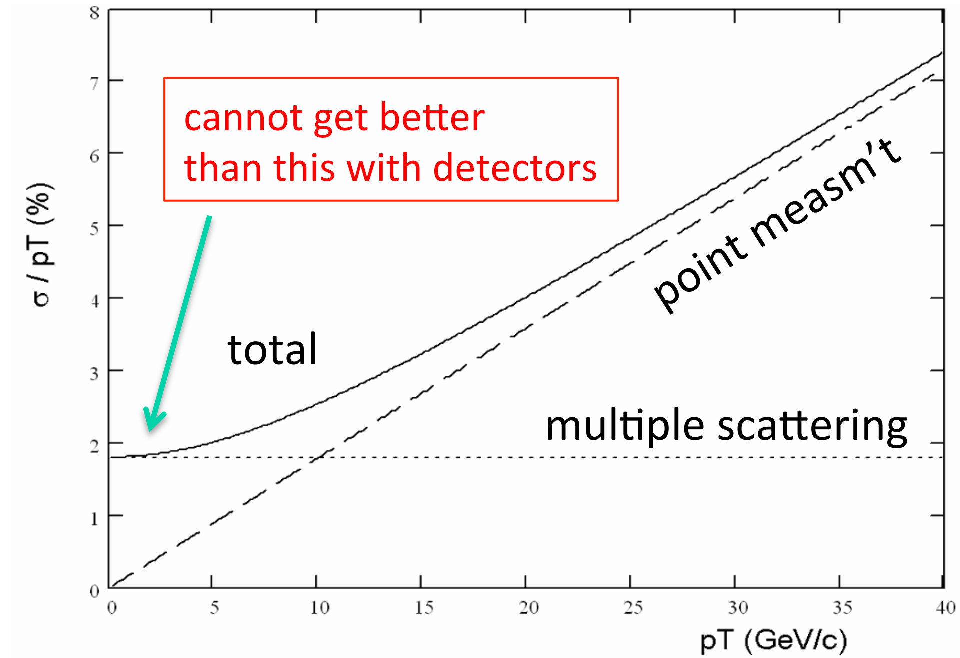

Concluding on σ_{d0} and σ_{pT} ... we should ...

- optimize σ_{meas} until other effects dominate (e.g. MS)
- $1/L^2$: the longer *L* the better
- place first plane as near as possible to the prod. point
- p_T linearly better with B-field strength (!) ... but more confusion if many tracks

Increasing N also improves the resolution, but only as 1/√N

The technology most often used is Si - detectors

PRO – high resolution σ_{meas} ~ 10 µm

CON - expensive
- small *N*
- small *L*
- small X_0 => large MS

PRO not mentioned in this context: high rate capability

Most tracking detectors are ionization detectors

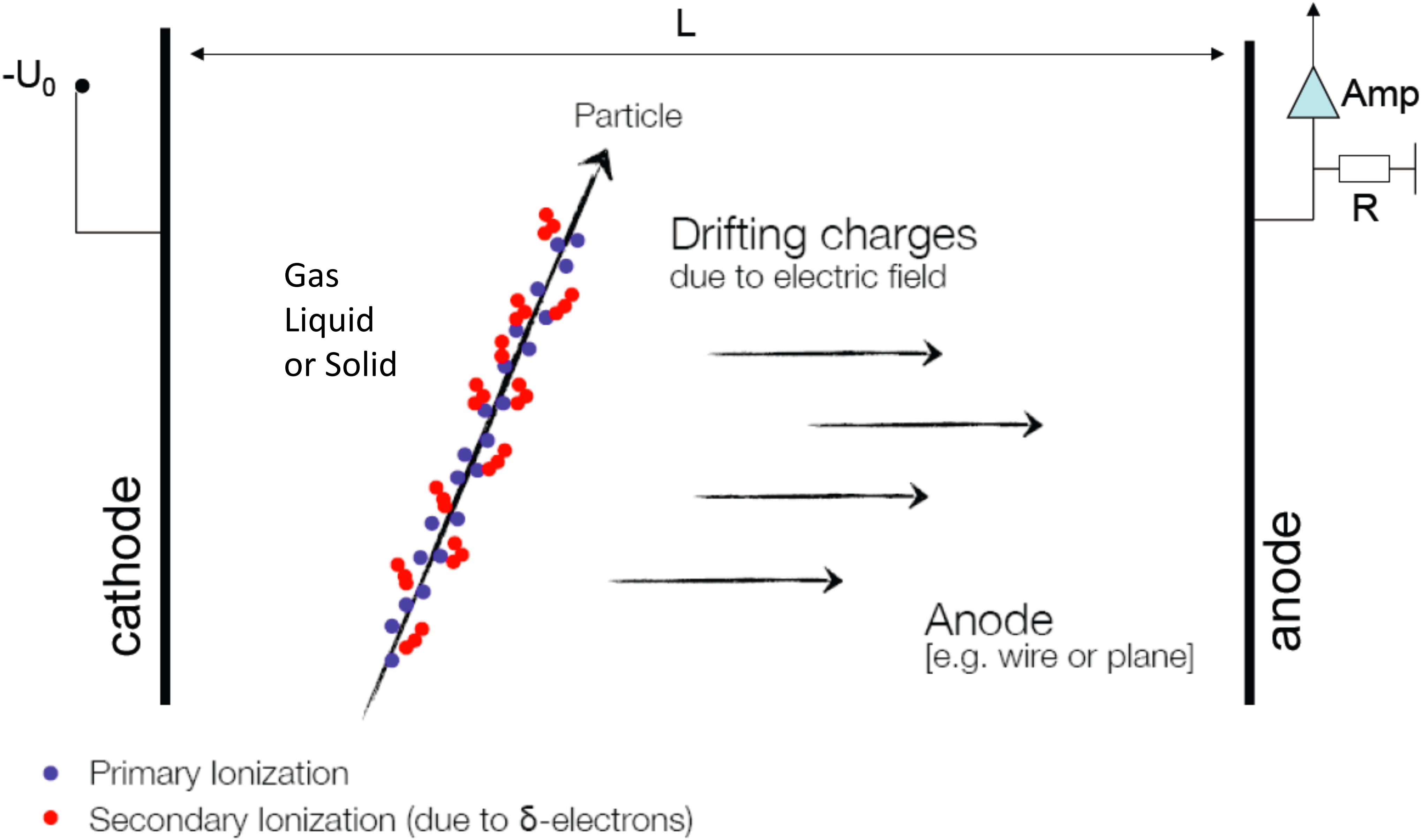

Ionisation energy loss

$$-\left\langle \frac{dE}{dx} \right\rangle = K \frac{Z}{A} \rho \frac{z^2}{\beta^2} \left[\frac{1}{2} \ln \frac{2\, m_e\, c^2\, \beta^2\, \gamma^2\, T_{max}}{I^2} - \beta^2 - \frac{\delta(\beta\gamma)}{2} - \frac{C(\beta\gamma,\, I)}{Z} \right]$$

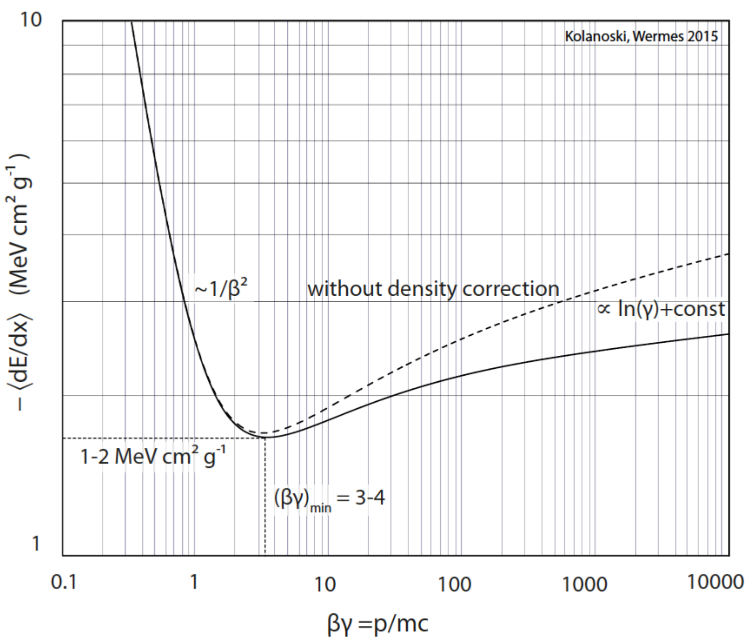

- does almost NOT depend on material (Z/A ≈ ½, ln I)
- proportional to z^2
- depends on βγ = p/E * E/m = p/m of projectile
- same curve for all z=1 particles when plotted as a function of βγ
- minimum at βγ=p/m = 3-3.5 (v=96%c)
- height of the plateau ~ 1.1 (solid) – 1.6 (gas) x minimum

- get different curves when plot against p (momentum) -> possibility for particle identification

For trackers: gas-filled and semiconductor detectors

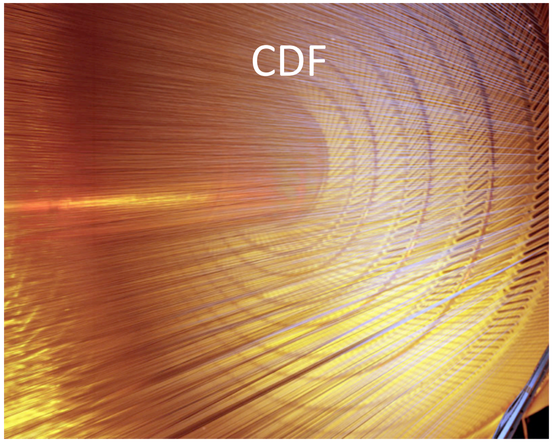

++	material	-
+	N_{meas}	--
low	cost	high
--	rate/speed	++
100 μm	resolution	10 μm

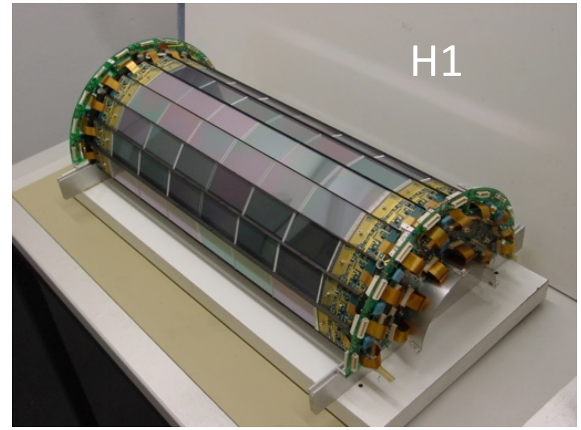

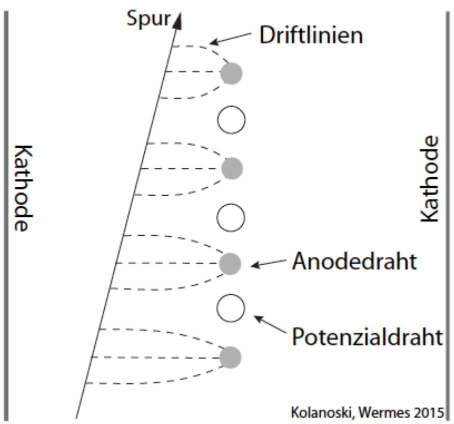

field near wire
$E(r) \sim 1/r$

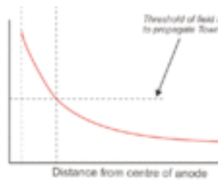

⇒ gas amplification

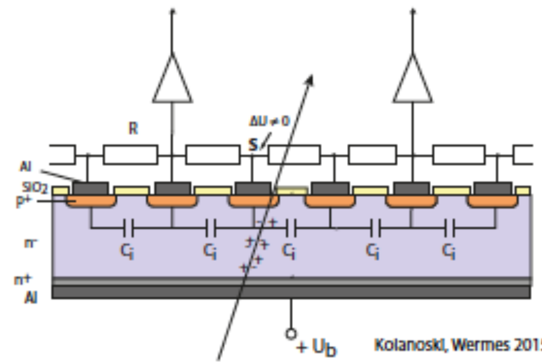

linear E

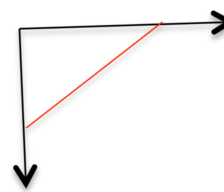

26 eV needed (Ar) per e/ion pair
94 e/ion pairs per cm
intrinsic amplification typ. 10^5
typ. noise: > 3000 e- (ENC)

3.65 eV (Si) needed per e/h pair
~10^6 e/h pairs per cm (20 000/250μm)
no intrinsic amplification
typ. noise: 100 e- (pixels) to 1000 e- (strips)

How the signal develops

by "electrostatic induction"

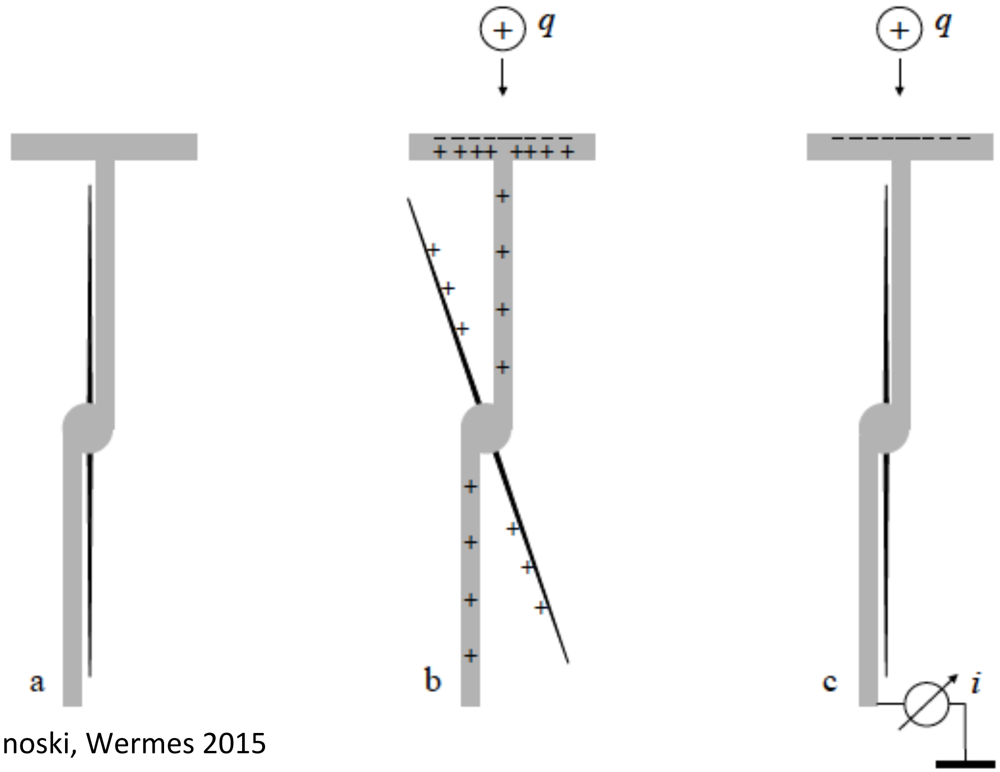

Kolanoski, Wermes 2015

a current is generated

Signal generation in an electrode configuration

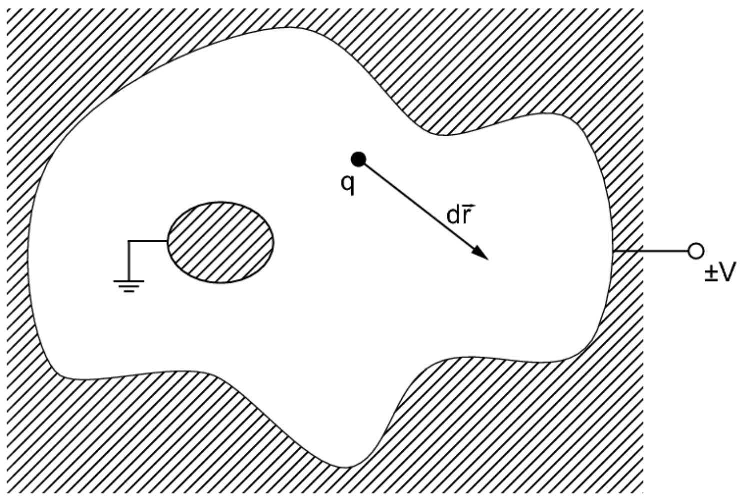

how does a moving charge couple to an electrode ?

- respect Gauss' law and find

Shockley- Ramo theorem
(Shockley J Appl.Phys 1938, Ramo 1939)

weighting field
determines how charge movement couples to a specific electrode

$$i_S = -\frac{dQ}{dt} = q\,\vec{E}_w\,\vec{v}$$

$$dQ = q\vec{\nabla}\Phi_W\,d\vec{r}$$

induction (weighting) potential
determines how charge movement couples to a specific electrode

Ramo Theorem in a many electrode configuration

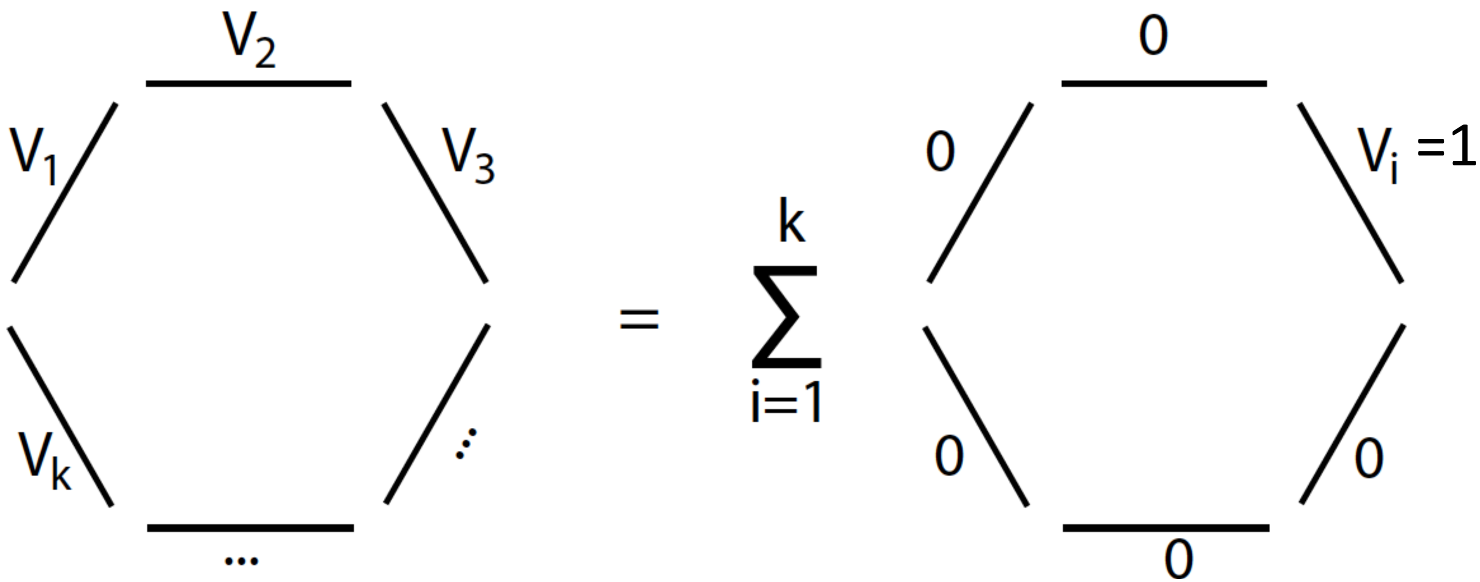

$$dQ_i = -q\,\vec{E}_{w,i}\,d\vec{r}$$

Recipe: To compute the weighting field of a readout electrode i, set voltage of electrode i to 1 and all other electrodes to 0.

Normal Field and Weighting Field

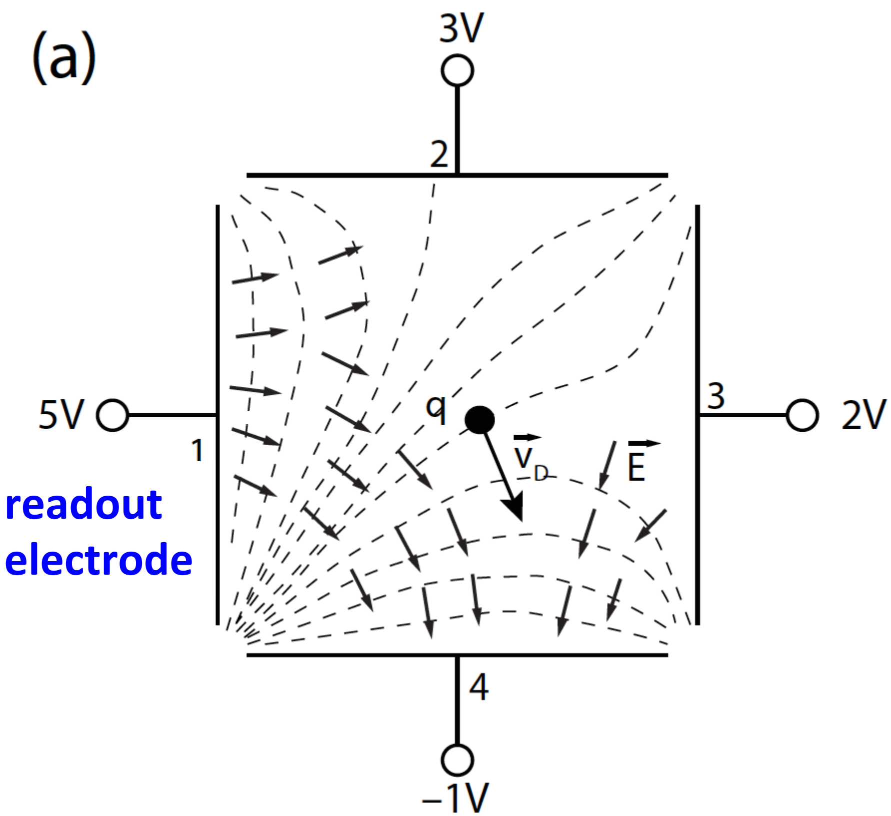

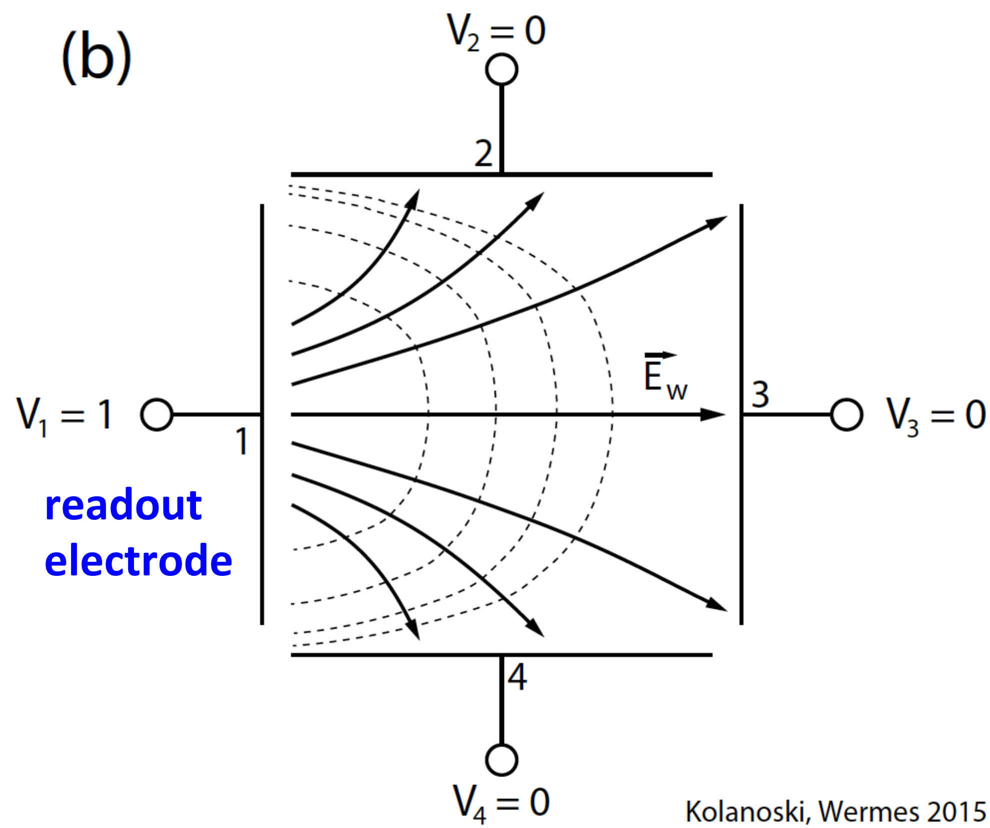

Kolanoski, Wermes 2015

$$i_S = -\frac{dQ}{dt} = q\,\vec{E}_w\,\vec{v}$$

A detector is a **current source**

delivers a current pulse
independent of the load

one can convert current into
charge (integral) or voltage (via R or C)

A parallel plate detector (capacitor)

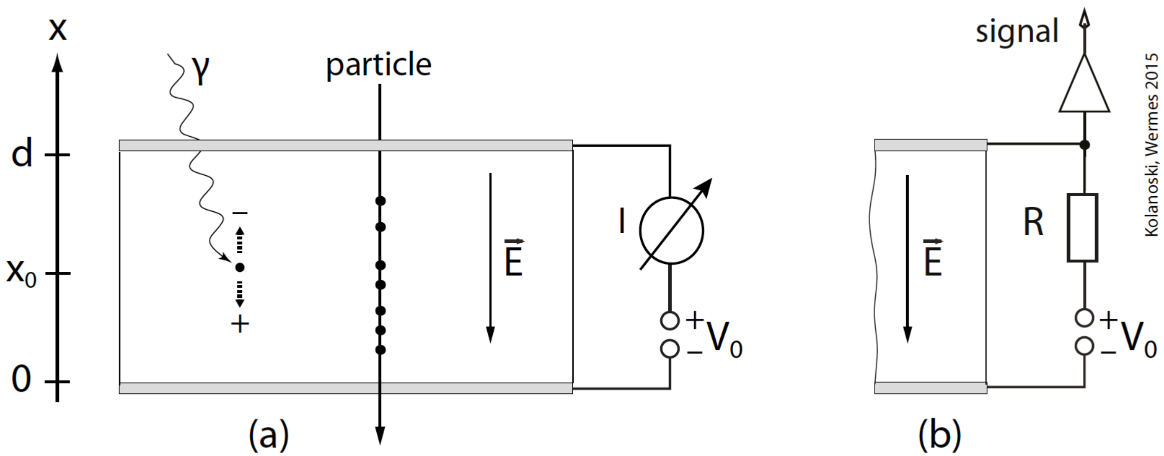

$$\vec{E} = -\frac{V_0}{d}\vec{e}_x \ , \qquad C = \frac{\epsilon\epsilon_0 A}{d}$$

- constant E-field
- almost constant velocity (v=μE)
- weighting field is simple

$$\vec{E}_w = -\frac{1}{d}\vec{e}_x$$

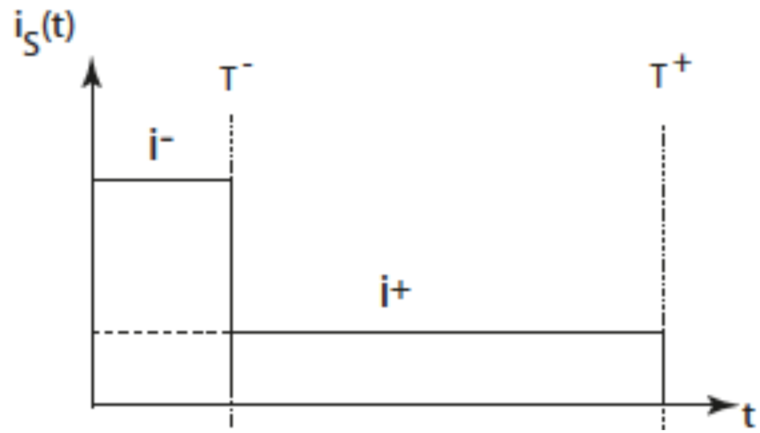

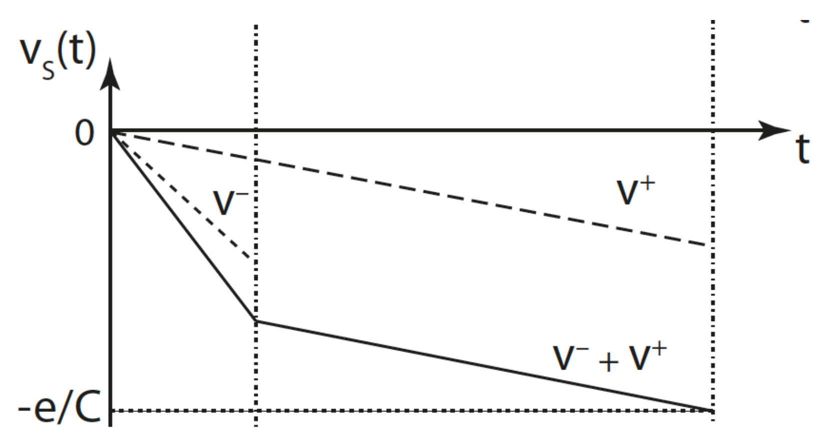

$$i_S^{\pm} = q^{\pm}\vec{E}_w\,\vec{v}^{\pm} = -\frac{q^{\pm}}{d}\,\vec{e}_x\,\vec{v}^{\pm} = \frac{e}{d}v^{\pm}$$

$$Q_S^{tot} = Q_S^- + Q_S^+ = -\frac{e}{d}\left(\int_0^{T^-} v^- dt + \int_0^{T^+} v^+ dt\right)$$

$$= -\frac{e}{d}v^-\left(\frac{d - x_0}{v^-}\right) - \frac{e}{d}v^+\left(\frac{x_0}{v^+}\right) = -e\,.$$

Signal in a Silicon detector (= parallel plate w/ space charge)

universitätbonn

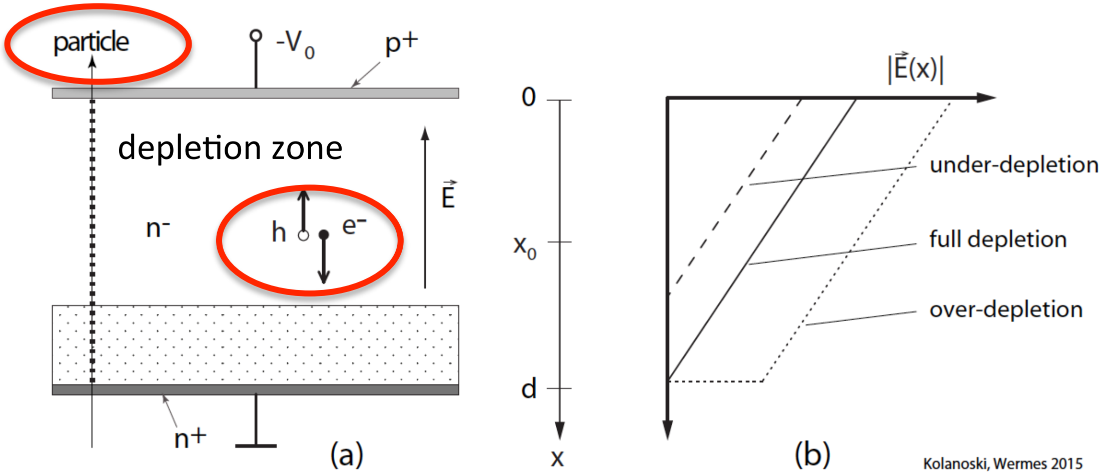

- E-field not constant
- velocity not constant
- weighting field still the same

$$\vec{E}_w = -\frac{1}{d}\vec{e}_x$$

$$\vec{E}(x) = -\left[\frac{2V_{dep}}{d^2}(d-x) + \frac{V - V_{dep}}{d}\right]\vec{e}_x \;=-\left[\frac{V + V_{dep}}{d} - \frac{2V_{dep}}{d^2}x\right]\vec{e}_x$$

$$v_e = -\mu_e E(x) = +\mu_e\,(a - bx) = \dot{x}_e$$
$$v_h = +\mu_h E(x) = -\mu_h\,(a - bx) = \dot{x}_h$$

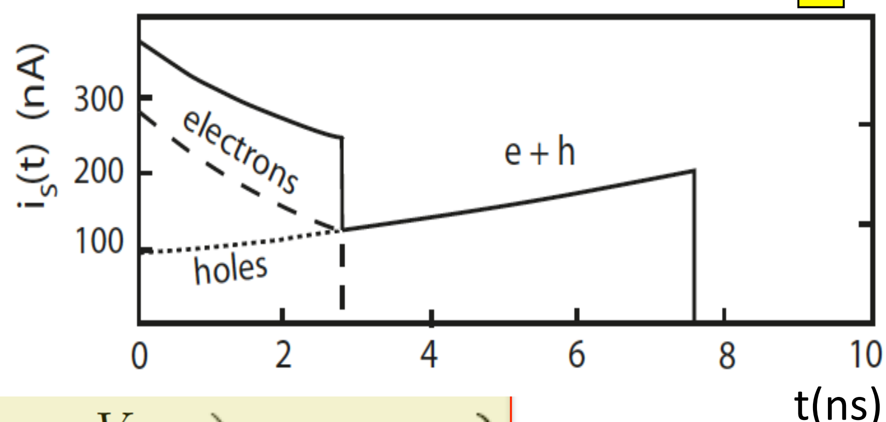

$$i_S(t) = i_S^e(t) + i_S^h(t)$$
$$= -\frac{e}{d}\left(\frac{2V_{dep}}{d^2}\,x_0 - \frac{V + V_{dep}}{d}\right)$$
$$\times\left\{\mu_e \exp\left(-2\mu_e\frac{V_{dep}}{d^2}t\right)\Theta(T^- - t) - \mu_h \exp\left(+2\mu_h\frac{V_{dep}}{d^2}t\right)\Theta(T^+ - t)\right\}$$

Current and charge signals

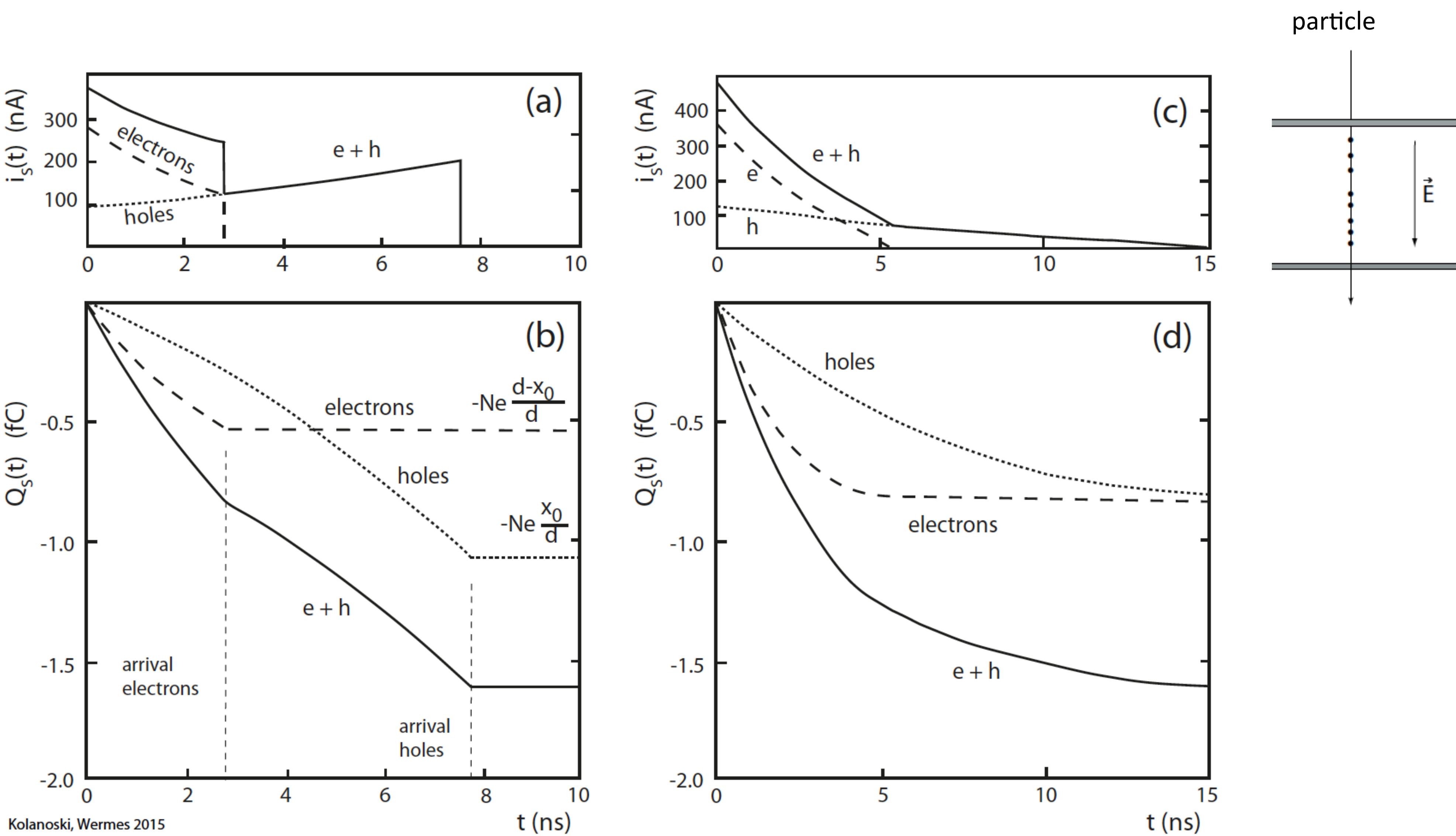

Kolanoski, Wermes 2015

transient current

Current pulse measurements: TCT technique

universitätbonn

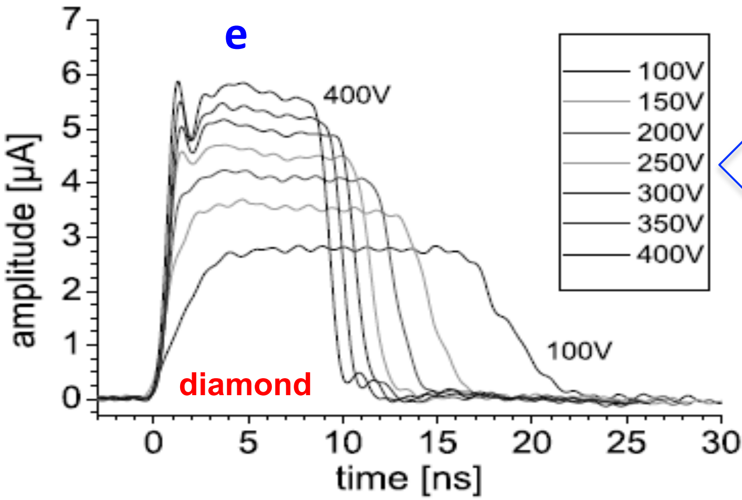

single crystal **diamond** is like a parallel plate detector filled with a dielectric w/o space charge

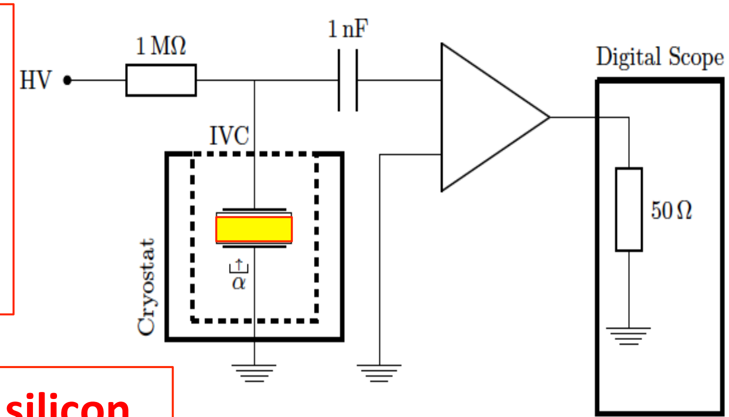

1mm pn – Diode **silicon**

- same weighting field
- different electric field

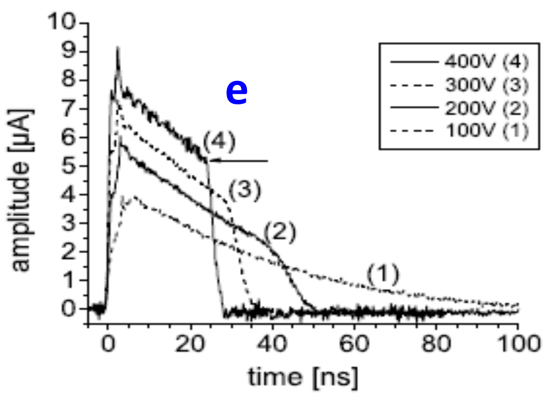

(a) Electron signals from α-particles impinging on the cathode.

Si

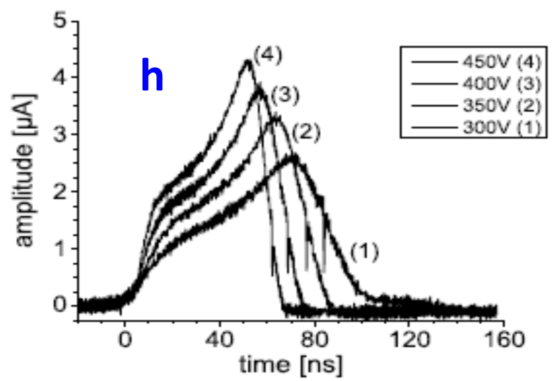

(b) Hole signals from α-particles impinging on the anode.

=>

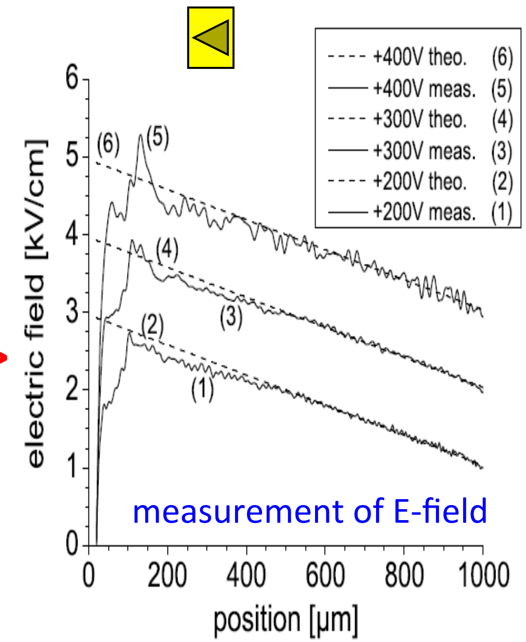

Note

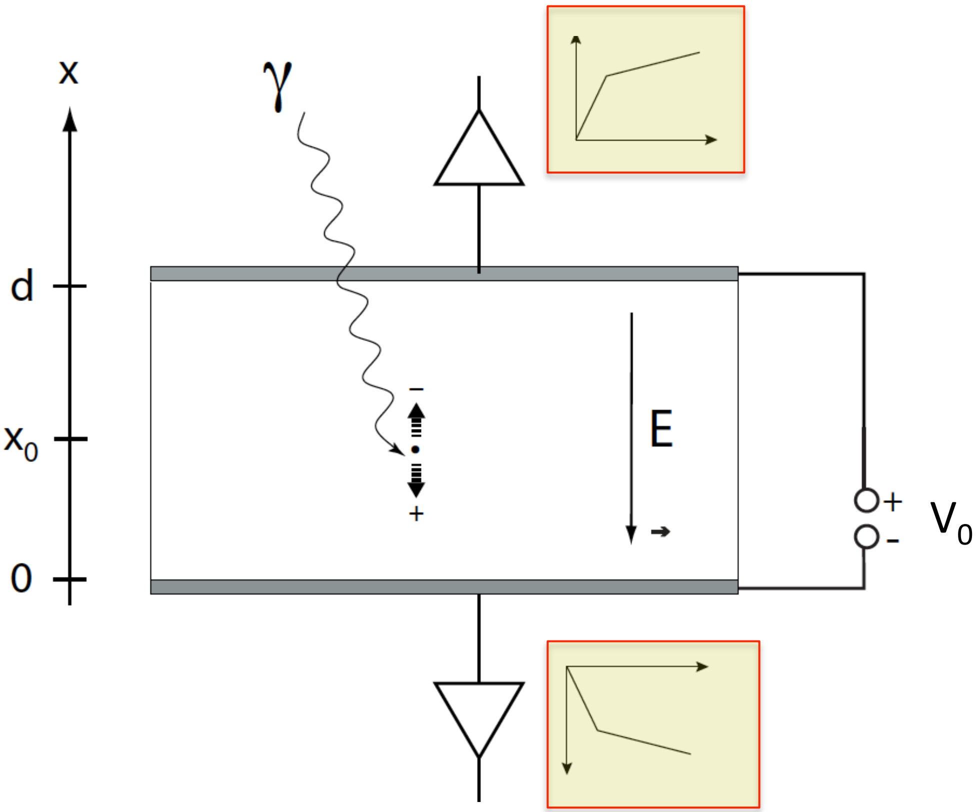

- movement of both charges create signals on both electrodes.
- on every electrode a total charge of

$$Q_S^{tot} = Q_S^- + Q_S^+ = -Ne$$

is induced.

- if a material the produced charges have very different mobilities (like CdTe) e.g. with $\mu_h \approx 0$, then part of the signal is lost and the signal becomes dependent on where the charge was deposited.

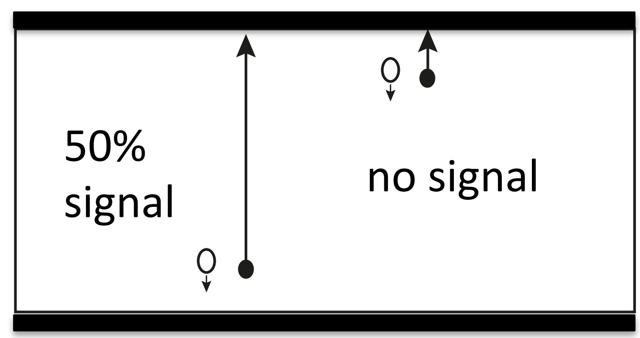

Signal development in a wire chamber

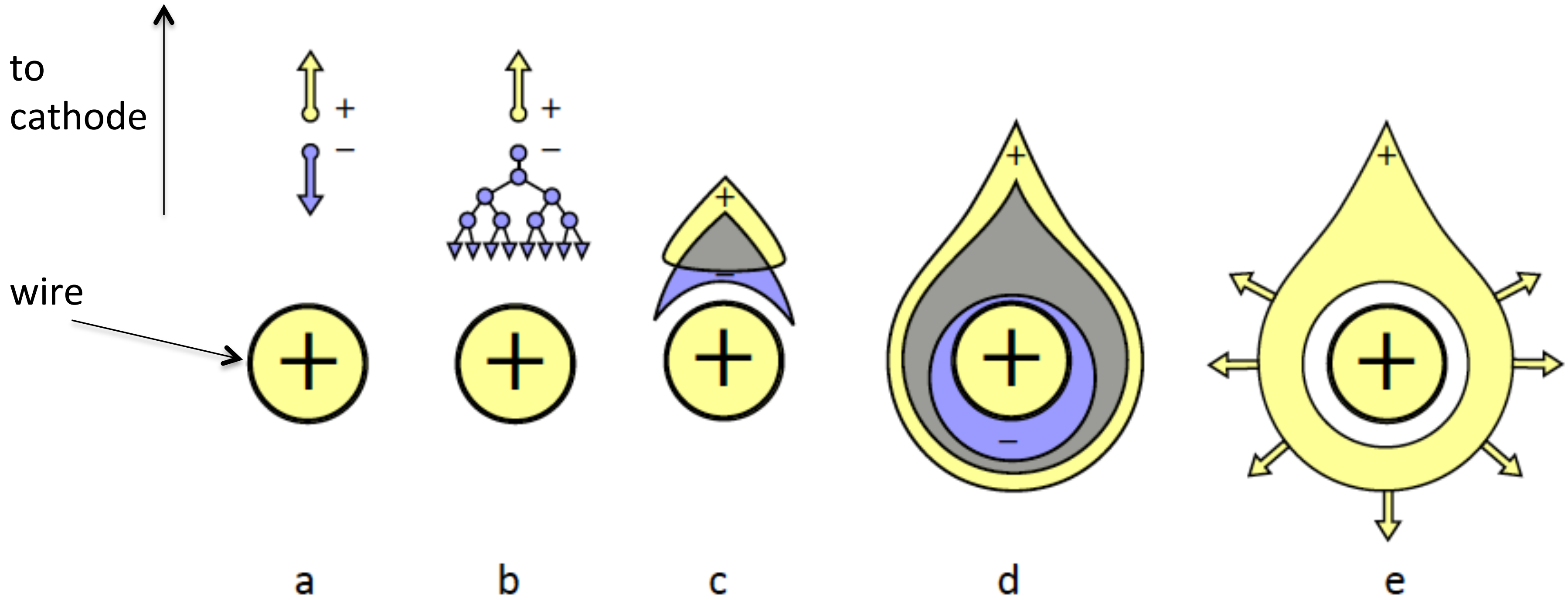

big difference:

- electrode (wire) does not "see" (too small) the charge before gas amplification
- signal (on wire) shape is governed by the (large) ion cloud moving away from the wire to cathode

Avalanche process:

$$dN = \alpha(E)\, N\, ds$$

with

$$\alpha = \sigma_{ion}\, n = \frac{1}{\lambda_{ion}}$$

1st Townsend coefficient

$$N(x) = N_0 e^{\alpha x}$$

gas gain

$$\frac{N}{N_0} = G = e^{\alpha x}$$

Signal development in a wire configuration (1)

configuration

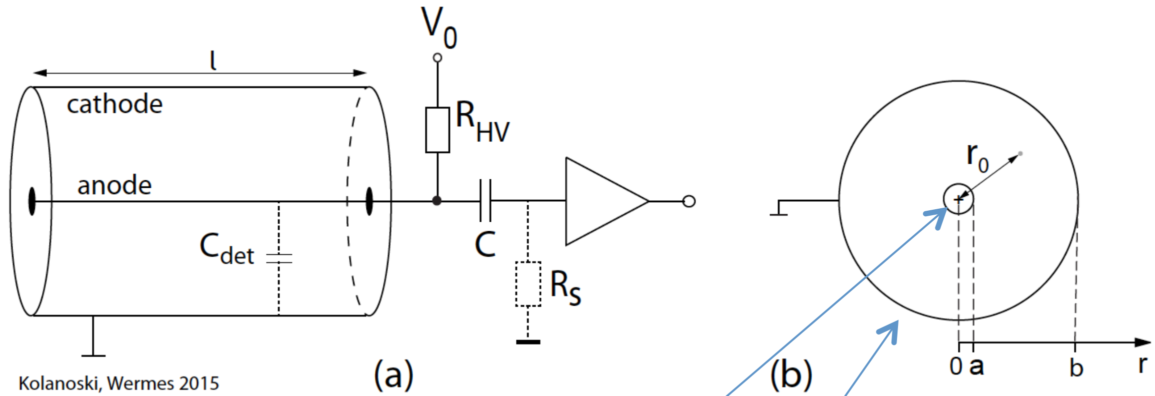

$$\vec{E}(r) = \frac{1}{r}\frac{V_0}{\ln b/a}\frac{\vec{r}}{r}, \qquad \phi(r) = -V_0\frac{\ln r/b}{\ln b/a}, \qquad C_l = \frac{2\pi\epsilon_0}{\ln b/a}$$

- we follow the Shockley-Ramo-recipe: find the weighting field E_W or the weighting potential Φ_W by setting

$$\phi_w(a) = 1\,, \quad \phi_w(b) = 0 \quad (*)$$

- we know already the shape of $\Phi_W \sim \ln r$, since $E(r) \sim 1/r$
- hence

$$\vec{E}_w(r) = \frac{1}{r}\frac{1}{\ln b/a}\frac{\vec{r}}{r}, \qquad \phi_w(r) = -\frac{\ln r/b}{\ln b/a}$$

which fulfills (*)

Signal development in a wire configuration (2)

universitätbonn

- now use Shockley-Ramo $dQ_S = -q\vec{E}_w d\vec{r}$

- we assume that N e/ion-pairs are produced at r = r_0. Note that usually there is avalanche amplification (starting only in the high field region) and the vast majority of charges is produced very close to the wire (r_0 < 10 µm, see previous page)

- then we get immediately

$$Q_S^- = -(-Ne)\frac{1}{\ln b/a}\int_{r_0}^{a}\frac{1}{r}dr = -Ne\frac{\ln\ r_0/a}{\ln\ b/a}$$

$$Q_S^+ = -(+Ne)\frac{1}{\ln b/a}\int_{r_0}^{b}\frac{1}{r}dr = -Ne\frac{\ln b/r_0}{\ln b/a}$$

(**)

- and the total charge is $Q_S^{tot} = Q_S^- + Q_S^+ = -Ne$ ✔

- however, due to the 1/r dependence of the weighting field the situation is much different from that of a parallel plate detector: the contribution from electrons and ions is not necessarily the same but depends on r_0 (i.e where the avalanche is created) because only there N becomes large enough that the signal is "felt" by the electrode (wire).

Signal development in a wire configuration (3)

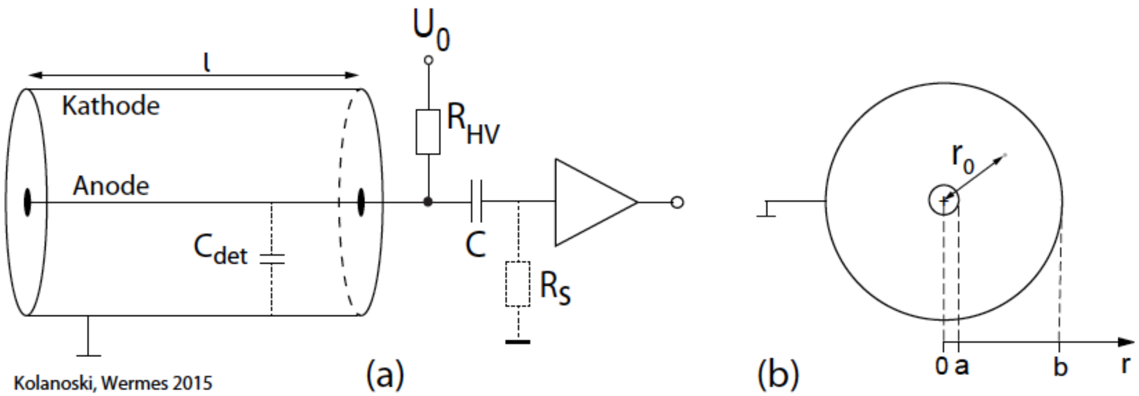

ratio depends on r_0

$$\left(\frac{Q_S^-}{Q_S^+}\right)_{r_0} = \frac{\ln r_0/a}{\ln b/r_0}$$

for a typical (a=10 µm, b=10 mm)

far away from wire

$$\left(\frac{Q_S^-}{Q_S^+}\right)_{r_0=b/2} \approx 9$$

near wire

$$\left(\frac{Q_S^-}{Q_S^+}\right)_{r_0=a+\epsilon} \approx 0.01 - 0.02$$

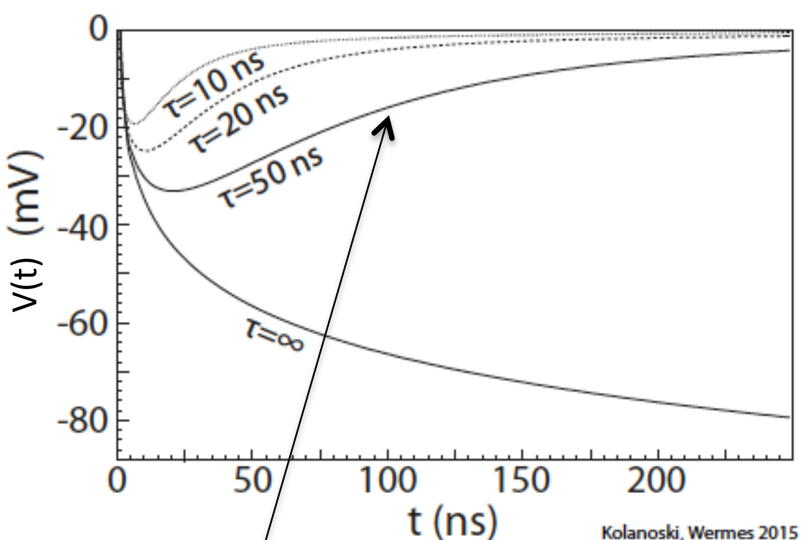

with RC filter

in wire chambers the (integrated) signal is dominated by the ion contribution. Reason: specific form of the weighting field

using Ramo and r(t) from the 1/r - E-field, we get …

$$i_S^+(t) = \frac{Ne}{2\ln b/a}\frac{1}{t+t_0^+}$$

ions only

$$v_s(t) = \frac{Q_S(t)}{C_l l} = \frac{Ne}{2\pi\epsilon_0 l}\ln\left(1+\frac{t}{t_0^+}\right)$$

Summary: Signal formation characteristics in a wire chamber

- electric field is large close to the wire @ $r \approx r_{wire}$
  => secondary ionization has a much larger effect on signal
  than primary ionization
  => avalanche near wire: $q \rightarrow q \times 10^{4\text{-}7}$

- from there (µm's away from wire) the electrons reach the wire fast
  => very small and fast e^- component of Q_{tot}

- ions move slowly away from wire => main component of $Q_{tot}(t)$

- signal only relevant after avalanche ionization ≅ quasi only $Q^+(t)$

- the term 'charge collection' is more justified in wire chambers than in other ionization detectors (e.g. parallel plate detectors) since most of the signal is created only very close to the wire

Cathode readout

signals are induced on BOTH (ALL) electrodes => exploit for second coordinate readout

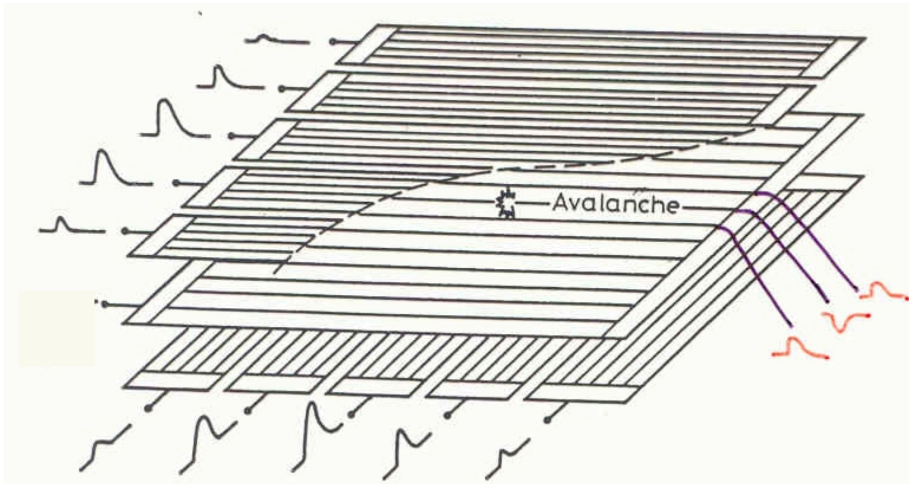

wire chamber
with cathode readout

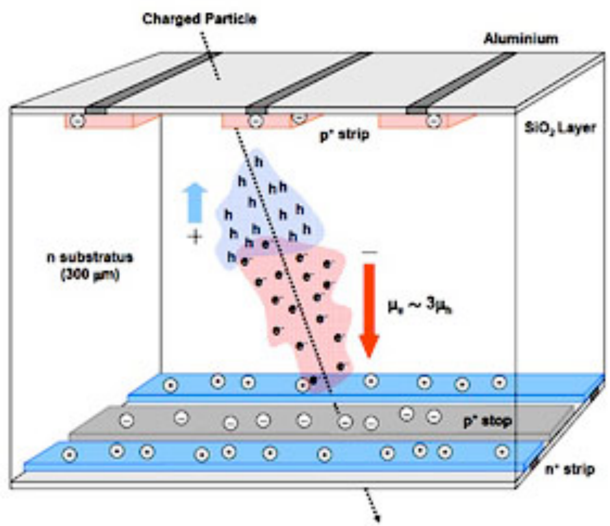

double sided
silicon strip detector

Signal generation in a patterned detector (1-dim)

universitätbonn

Φ_W for a strip/pixel geometry

$$\Phi(x,y) = \frac{1}{\pi}\arctan\frac{\sin(\pi y)\cdot\sinh(\pi\frac{a}{2})}{\cosh(\pi x)-\cos(\pi y)\cosh(\pi\frac{a}{2})}$$

(can be calculated e.g. by using “conformal mapping”)

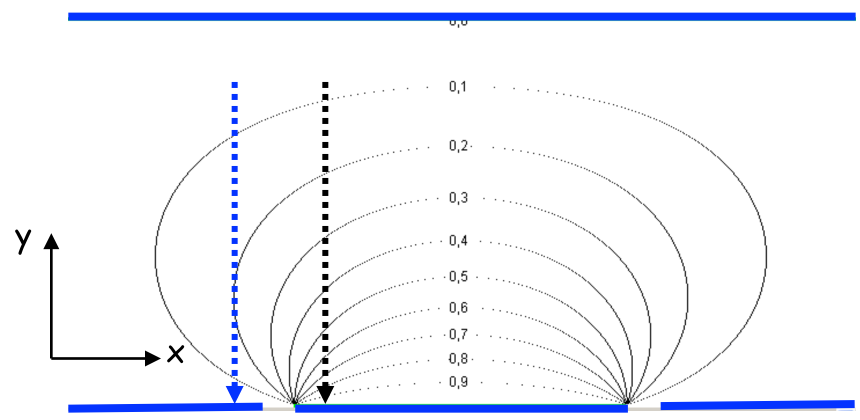

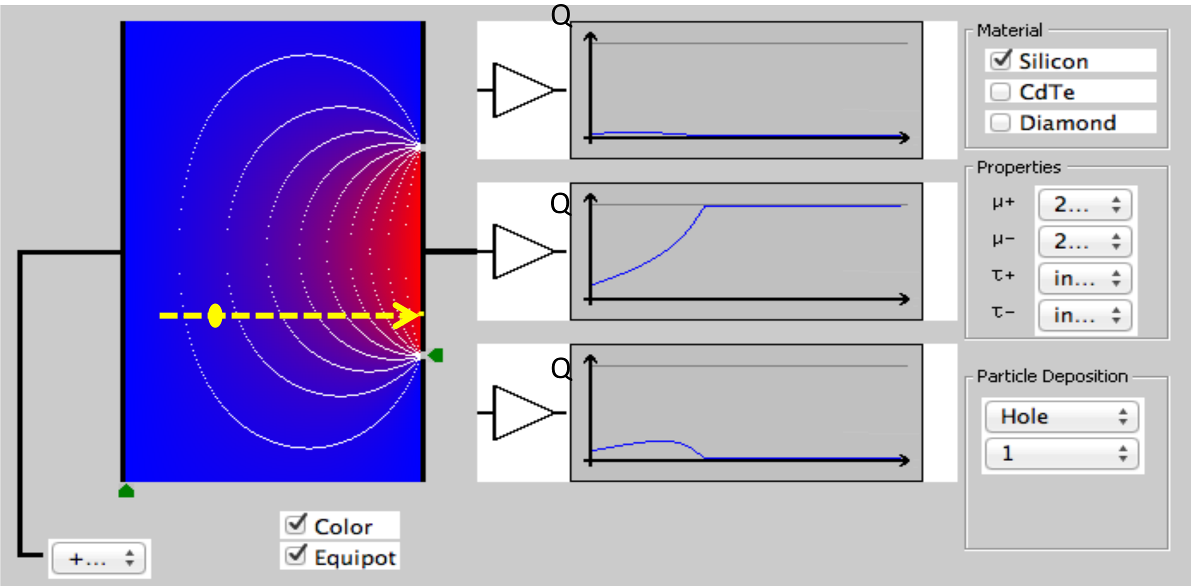

“small pixel effect” !

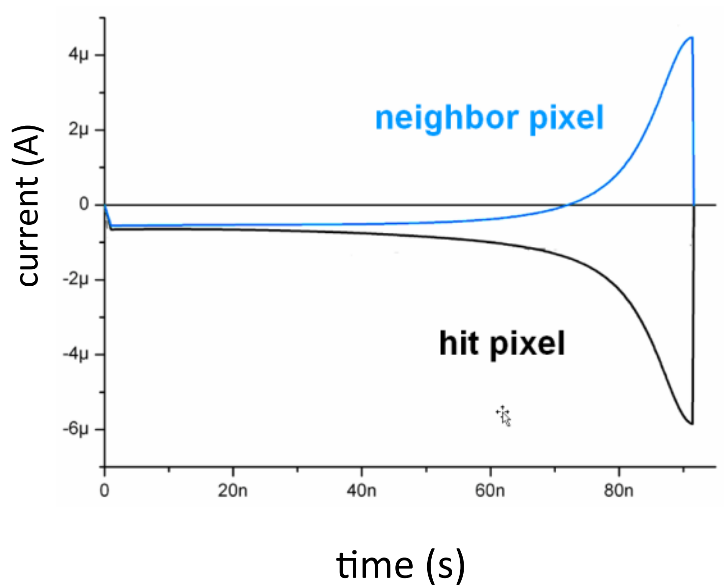

Concluding … consequences …

- The weighting field reaches also into regions of neighbor pixels → induced signals there as well
- At the beginning of the charge movement, neighbor pixels "see" almost as much signal as the "hit" pixel → no difference when electronics is (too) fast
- consequences for small electrodes is, that most of the charge is induced, when q is <u>near</u> the hit pixel → small pixel effect
- when charges drift only a short distance due to
  - $\mu_h << \mu_e$ (e.g. for CdTe)
  - trapping (e.g. for pCVD diamond)

  peculiar signal patterns may arise (worst case: holes do not move and electrons are trapped after 50 μm → several pixels "fire")

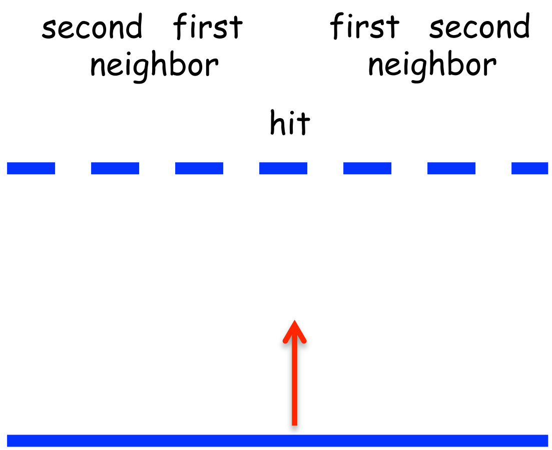

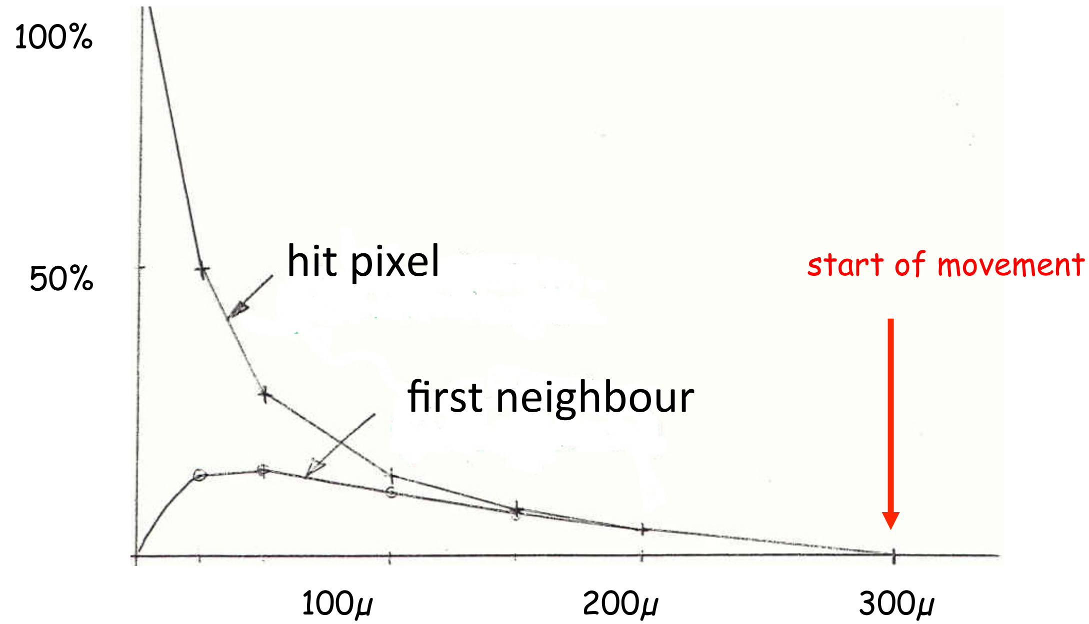

Diffusion and drift of charge cloud on way to electrode

E = 0, T > 0: diffusion

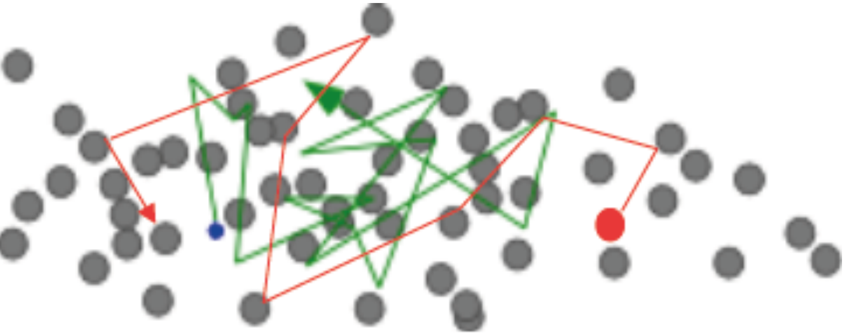

$$D = \frac{\langle \lambda v \rangle}{3} = \frac{1}{3\sigma p}\sqrt{\frac{8(kT)^3}{\pi m}}$$

E > 0, T > 0: diffusion + drift

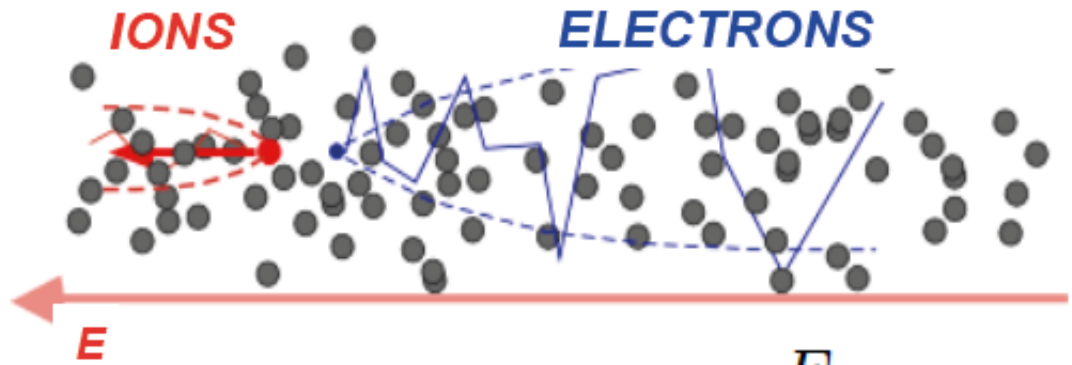

$$v_D = \mu(E)\, E = \frac{\mu_0 E}{\left[1 + \left(\frac{\mu_0 E}{v_{sat}}\right)^{\beta}\right]^{1/\beta}}$$

Drude ansatz (empirical)
(especially semiconductors)

β~1-2

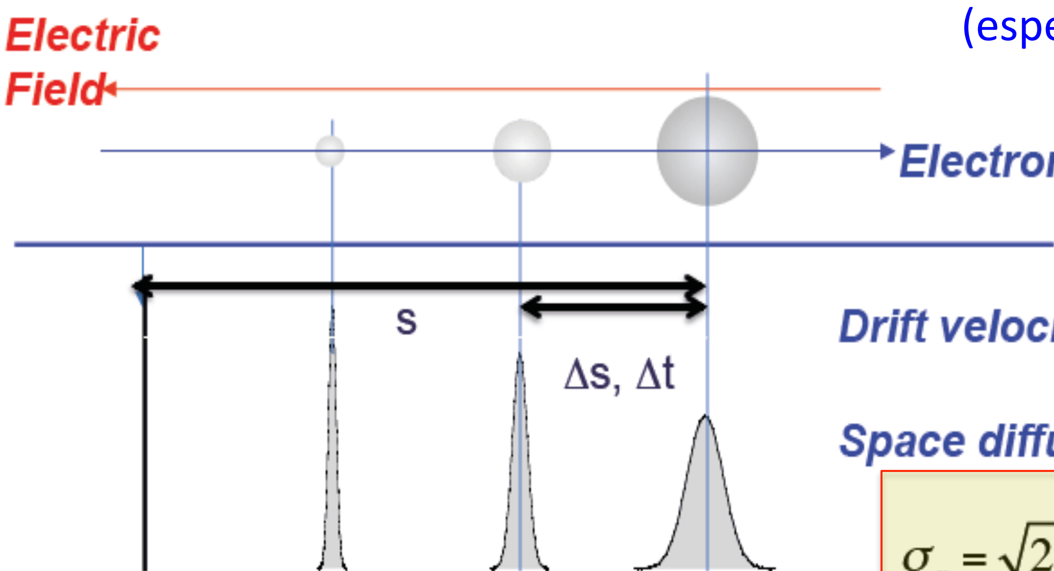

Drift velocity: $v_D = \frac{\Delta s}{\Delta t}$

Space diffusion rms:

$$\sigma_x = \sqrt{2Dt} = \sqrt{2D\frac{s}{v_D}}$$

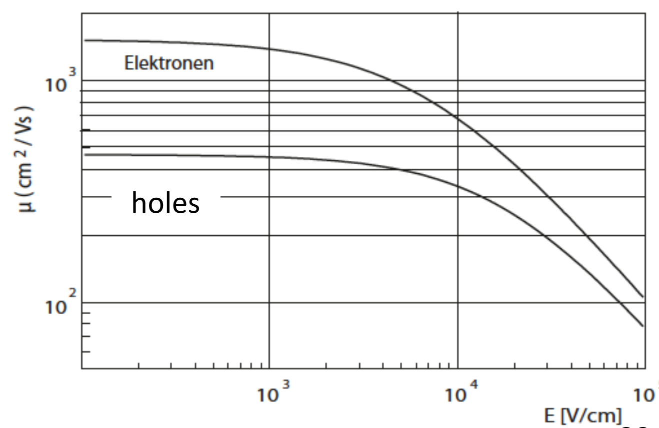

Movement in the presence of a magnetic field

universitätbonn

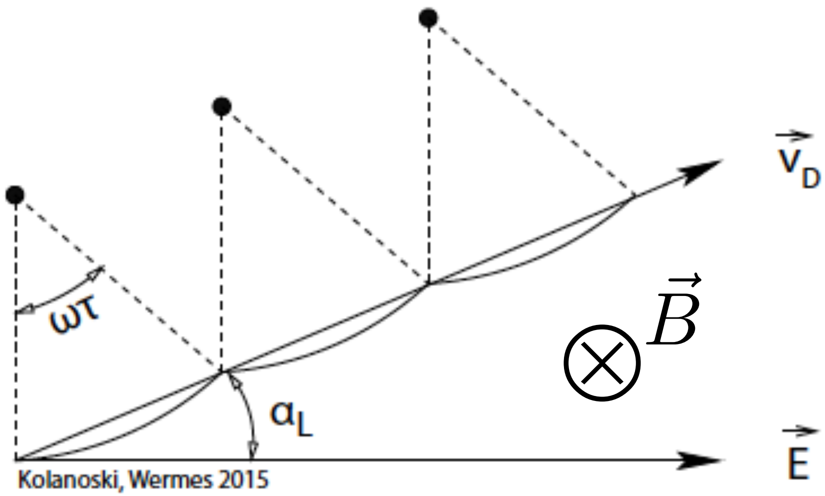

- if the electric field E is perpendicular to a magnetic field B then the charges drift on circle segments until they stop in a collision
- on average this results in a deflection of the drift path by an angle called

Lorentz angle

perp. to E

$$\tan \alpha_L = \frac{v_{D,\perp}}{v_{D,\parallel}} = \omega\tau$$

parallel to E

with

ω = qB/m = cyclotron frequency

τ = mean collision time

Spatial Resolution in segmented electrode configurations

remember Gluckstern formula

$$\left(\frac{\sigma_{p_T}}{p_T}\right)_{\text{mess}} = \frac{p_T}{0.3|z|}\frac{\sigma_{\text{mess}}}{L^2 B}\sqrt{\frac{720}{N+4}}$$

$$[p_T] = \text{GeV/c}, \; [L] = \text{m}, \; [B] = \text{T}$$

- binary readout (hit/no hit)
- analog readout (pulse height information)

- signal (charge) distributed on more than one electrode

binary R/O

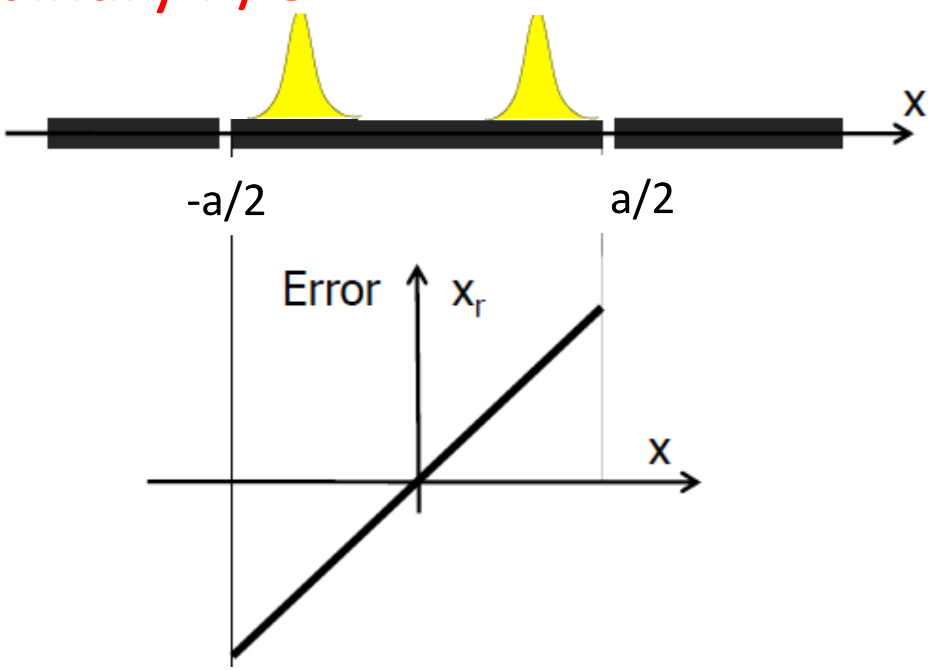

$$v = \int_{x_1}^{x_2} x^2 f(x)dx$$

$$\sigma_x^2 = \frac{1}{a}\int_{-a/2}^{a/2} \Delta_x^2 \, d(\Delta_x) = \frac{a^2}{12}$$

$$\sigma_x = \frac{a}{\sqrt{12}}$$

Spatial Resolution in segmented electrode configurations

universitätbonn

with analog information and spread over more than one electrode

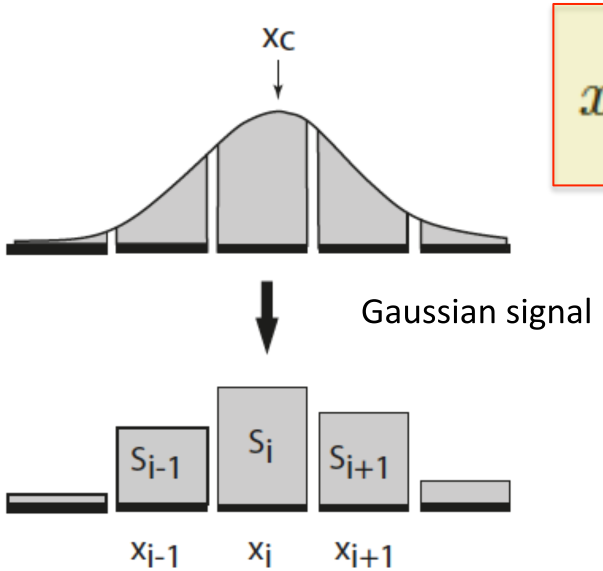

center of gravity

$$x_c = \frac{\sum S_i\, x_i}{\sum S_i}$$

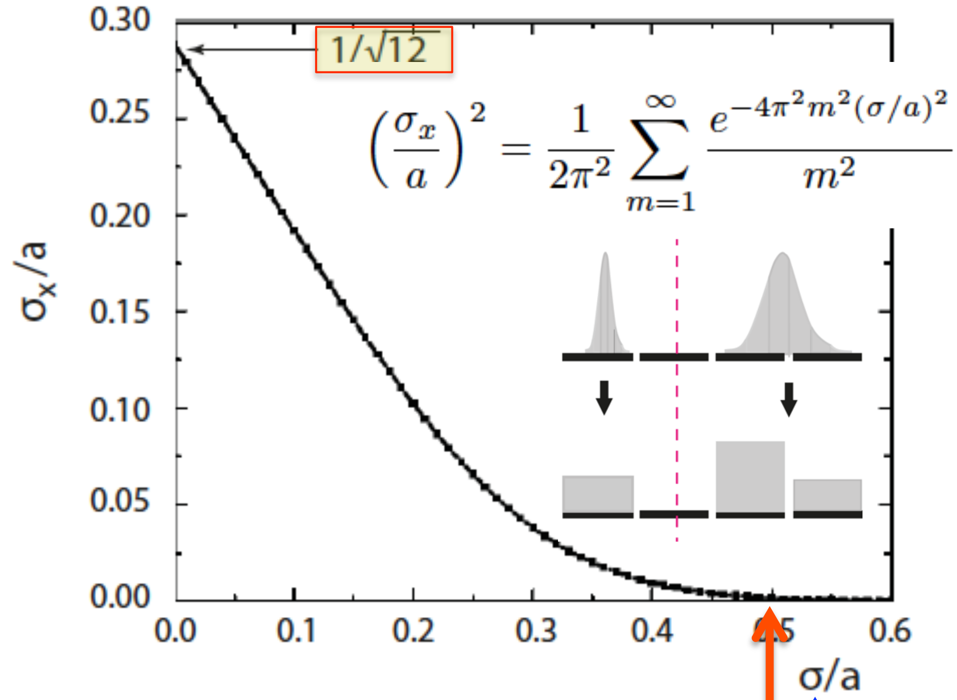

perfect resolution but only w/o noise

width of charge cloud

$$x_{rec} = \frac{\sum (S_i + n_i)\, x_i}{\sum (S_i + n_i)} = \frac{x + \sum n_i x_i}{1 + \sum n_i} = \left(x + \sum n_i x_i\right)\left(1 - \sum n_i + \mathcal{O}(n_i^2)\right)$$

with uncorrelated noise (normalized to signal)

$$\langle n_i^2 \rangle = \sigma_n^2, \quad \Rightarrow \sigma_x^2 = \sigma_n^2 \left[\left(\sum_{i=1}^{N} x_i^2 \right) + N \langle x^2 \rangle \right] + \mathcal{O}(\sigma_n^3)$$

Arbitrary detector response ("data driven method")

typical for semiconductor detectors
and patterned gaseous detectors
channels have different gains

$N_{electrodes}$ = 2-3, S/N ~ 10

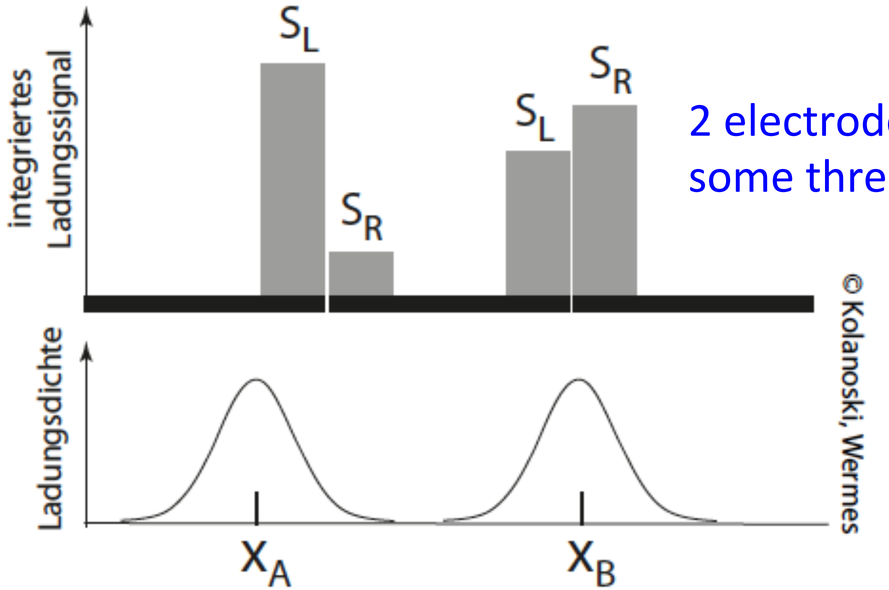

2 electrodes have signal over some threshold

$$S_L(x) = Q\,\eta(x)$$

$$S_R(x) = Q - S_L(x) = Q\,(1 - \eta(x))$$

η = response function, indep. of Q
can be determined from signals themselves

$$\eta = \frac{S_L}{S_L + S_R}$$

- assume a constant hit probability density
- => can build inverse of η-function (η -> x)
- pick best estimate of position from a measured distribution
- algorithm can also be extended to three – electrode situations

$$x_{rec} = \eta^{-1}\left(\frac{S_L}{S_L + S_R}\right) = \frac{a}{N}\int_0^{\eta} \frac{dN}{d\eta'} d\eta'$$

Arbitrary detector response

Belau, E. et al.: NIM 214 (1983) 253–260

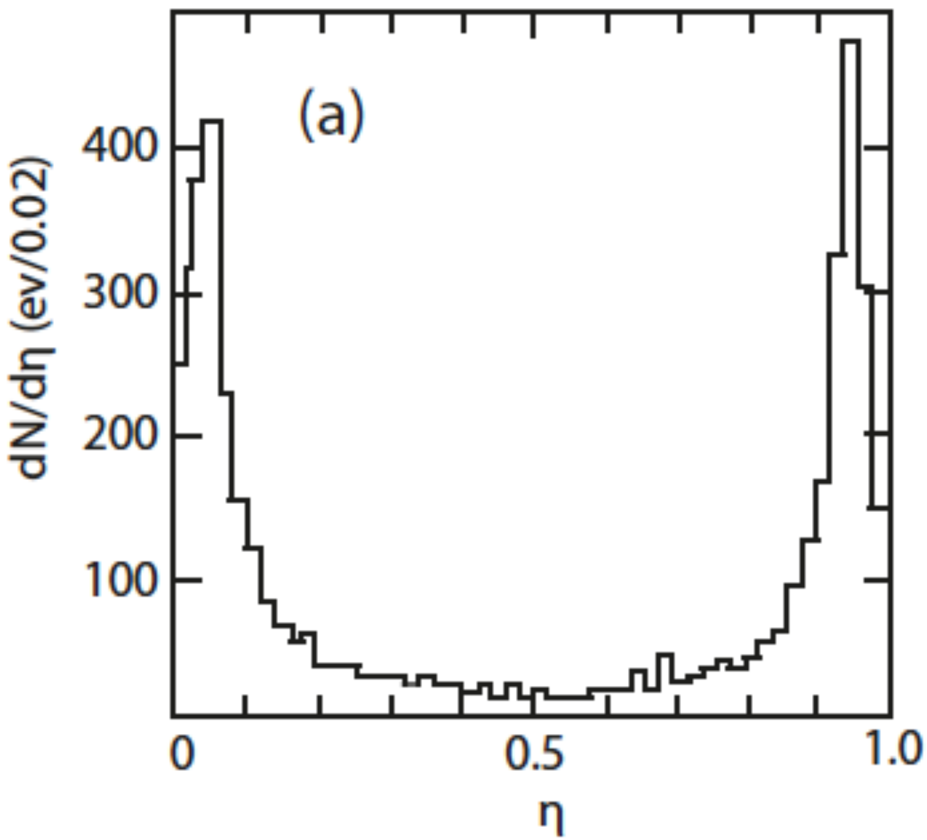

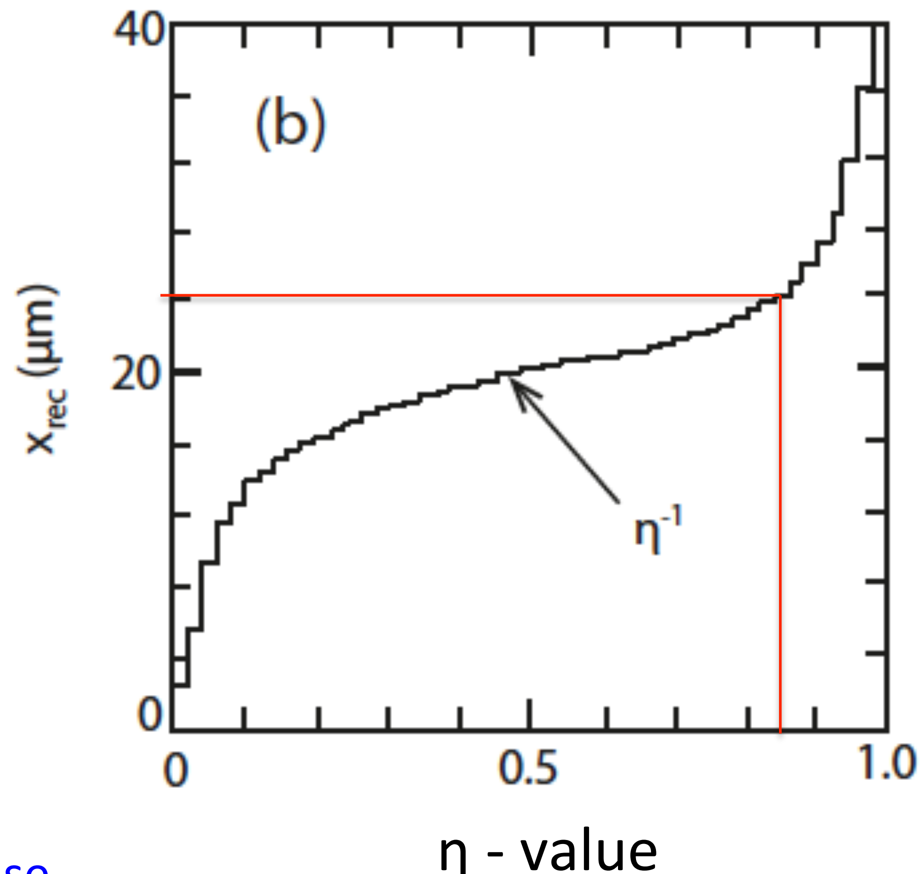

noise

resolution

$$\sigma_x^2 = 2\,\sigma_n^2 \left\langle \frac{\eta^2}{\eta'^{\,2}} \right\rangle$$

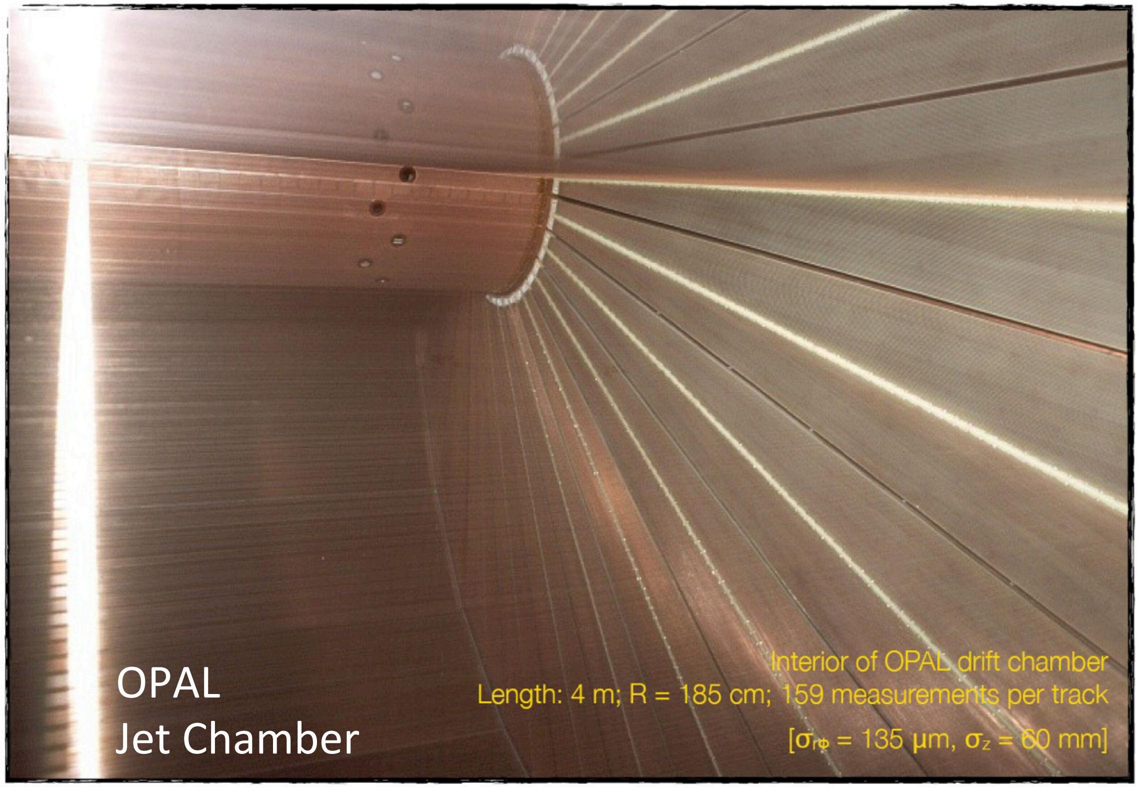

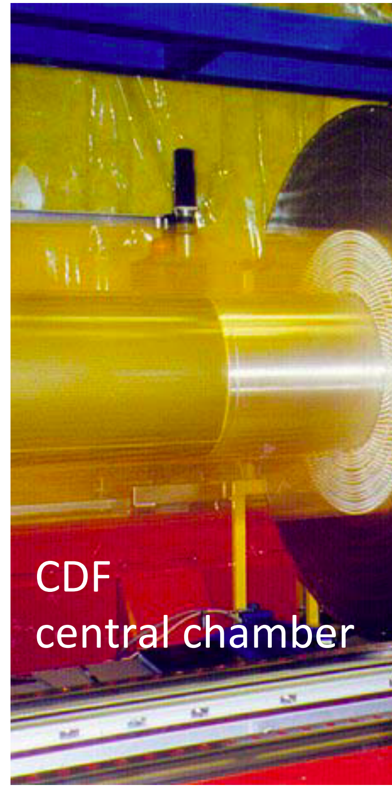

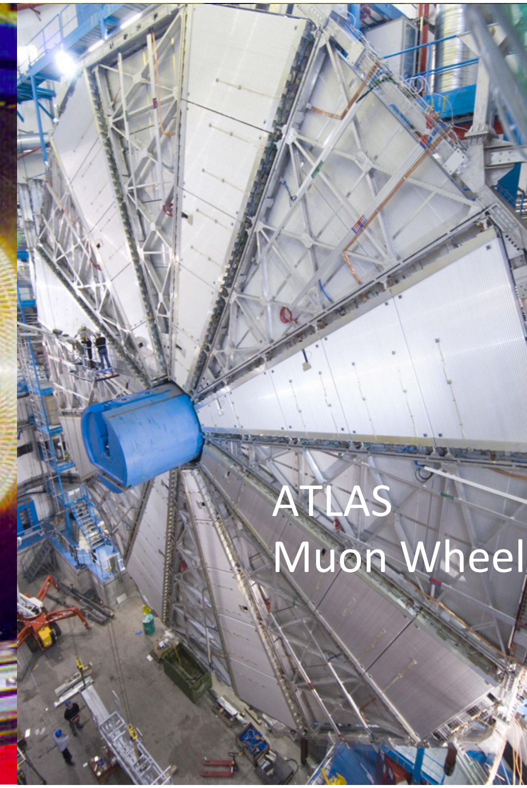

Gas-filled detectors

Multi Wire Proportional Chamber

universitätbonn

- mother of all wire chambers (1960ies)
- break through in tracking, because tracks became electronically recordable
- Nobel Prize 1992

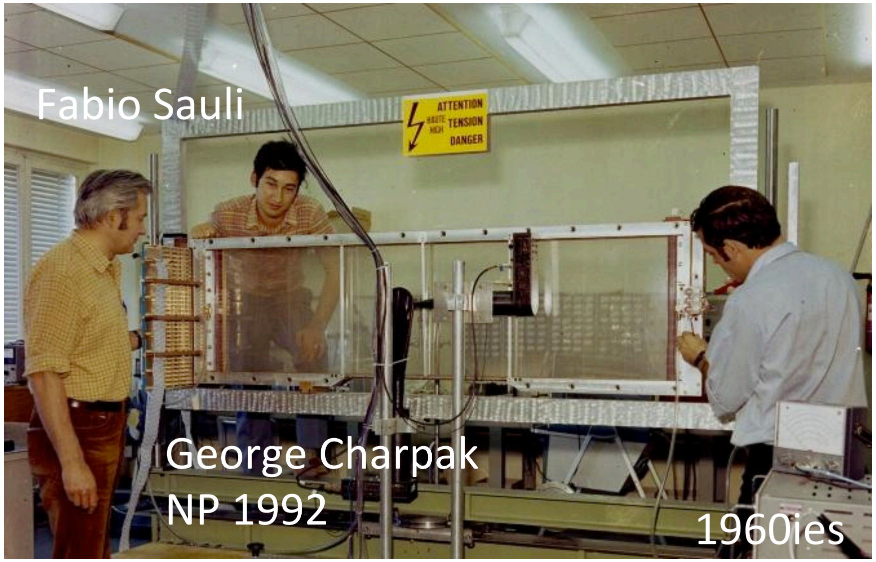

cathodes often patterned for 2nd coordinate

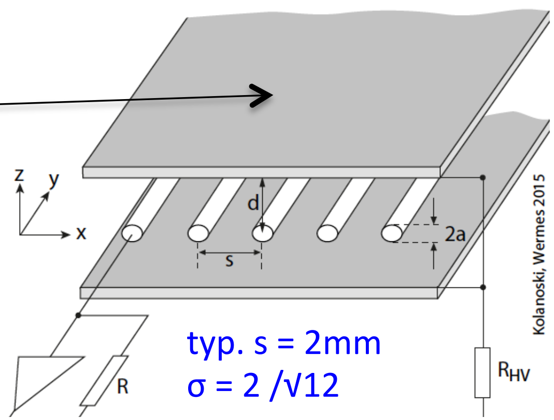

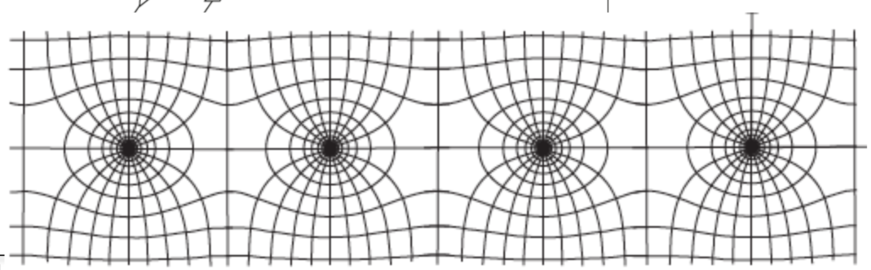

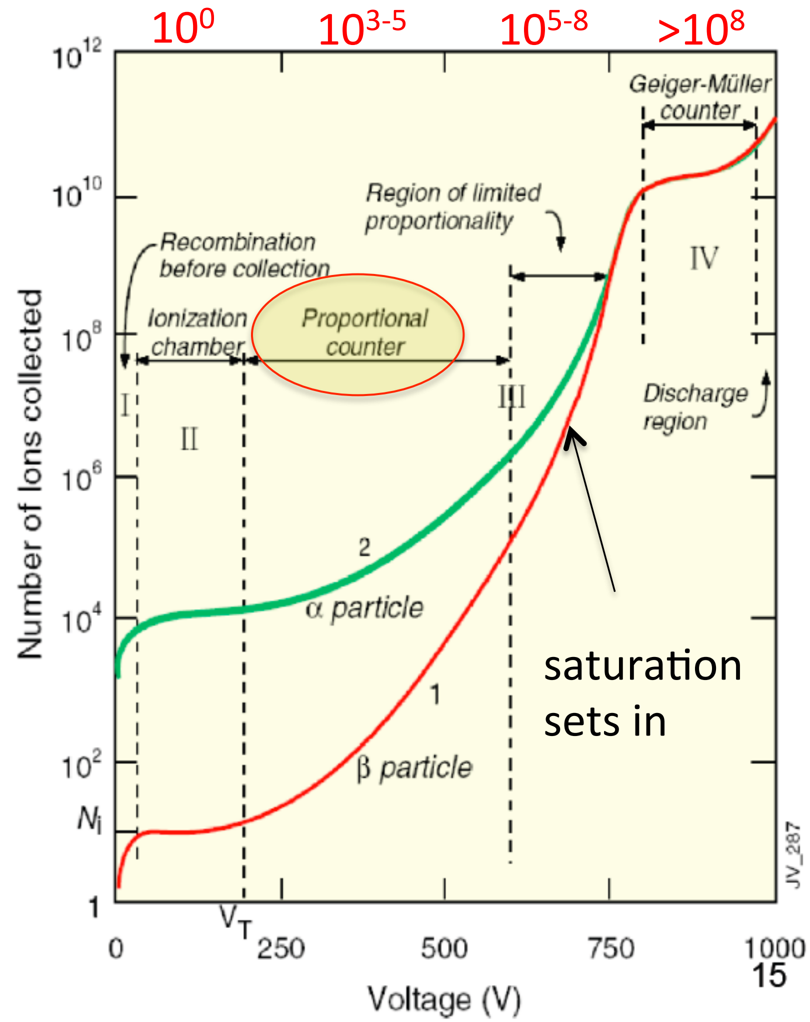

Operation modes of wire chambers

region of limited proportionality → multi wire chamber operation in saturation region (G ~10^5 - 10^7)

- operation point: gain > 10^6 → strong secondary ionization
- space charge effects (stationary ion cloud decreases the electric field at the anode) destroy 1/r shape near wire
- saturation of signal sets in

  this is sometimes wanted, when the number of particles is to be determined by the total signal height; e.g. when slow ($1/\beta^2$!) protons shall give the same signal height as m.i.p.s

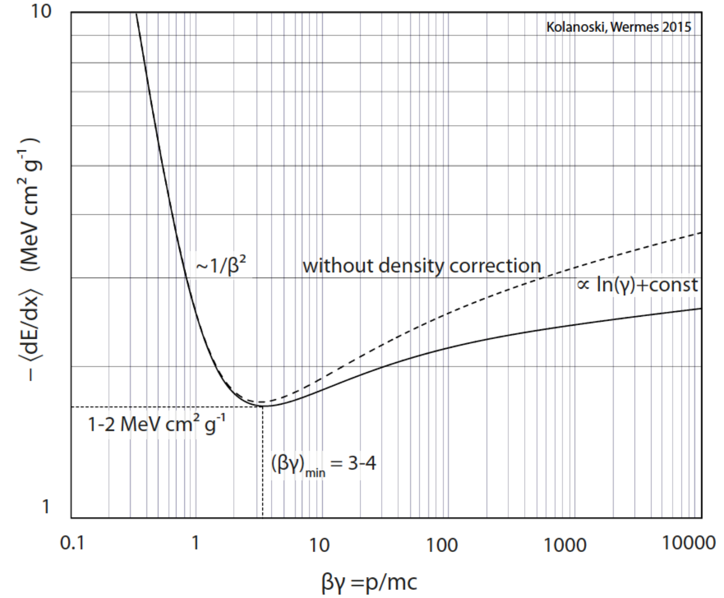

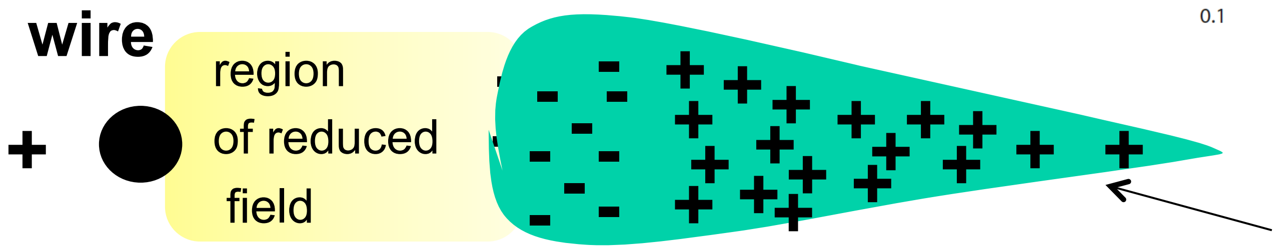

ion cloud is ~ stationary acts like a space charge

Saturation –> Avalanche –> Streamer –> Spark

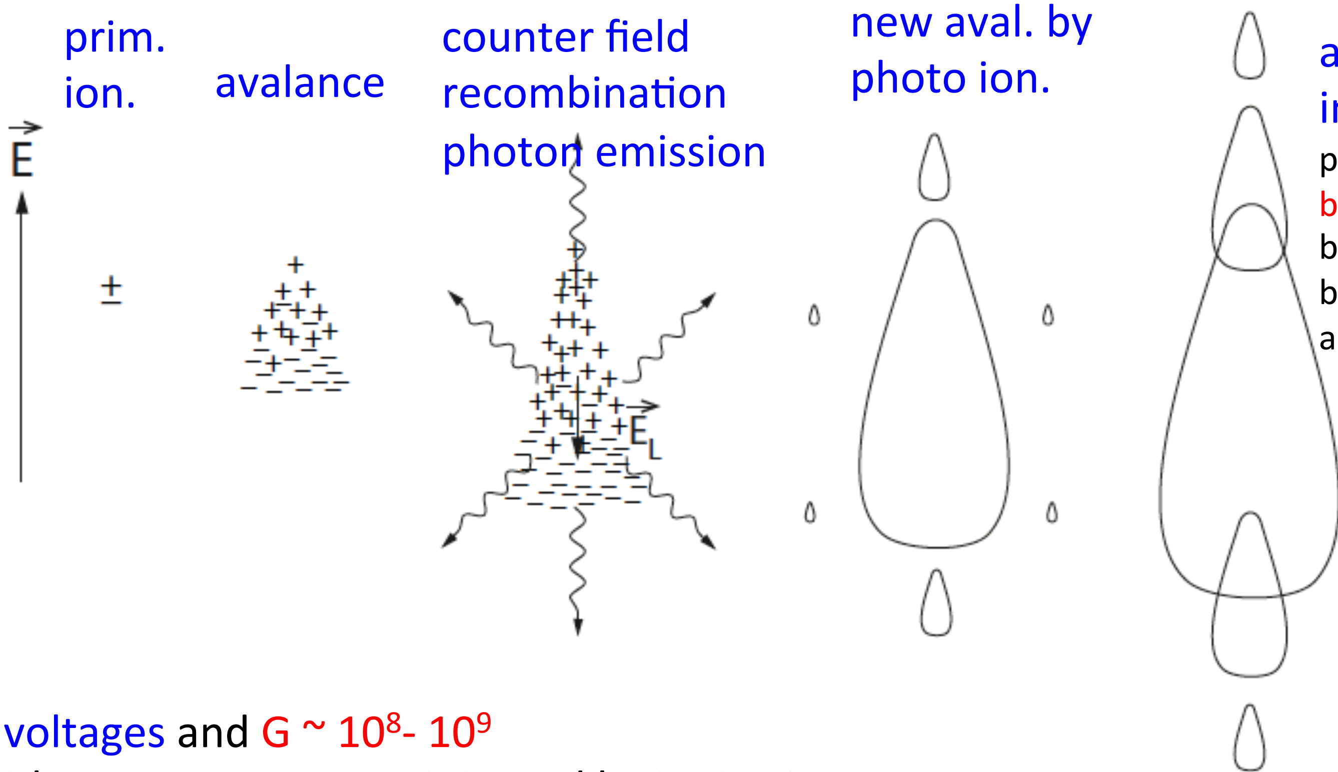

avalanches merge into a "streamer"
preferentially between electrodes because highest fields are between avalanche fronts and HV electrodes

- at very high voltages and $G \sim 10^8$- 10^9
- discharges either spontaneous or initiated by ionisation
- => saturated avalanche -> streamer -> discharge (= glow –> corona –> spark) occur
- streamer/discharge accompanied by photon emission (can be visible) and needs to be quenched (by HV-lowering, pulsed HV, space charge screening, etc.) when used as detectors rather than demonstration objects (spark ch.)
- very fast (10^6 m/s) governed by <u>photon emission</u>, 10x faster than avalanche dev. (governed by v_{drift})
- when streamer reaches electrode => spark/discharge => avoid in detectors (→limited streamer mode)
- (limited) streamer operation modes found today in straw tube geometries or RPCs

The second coordinate

cathode readout (see page 24) or crossed wire planes

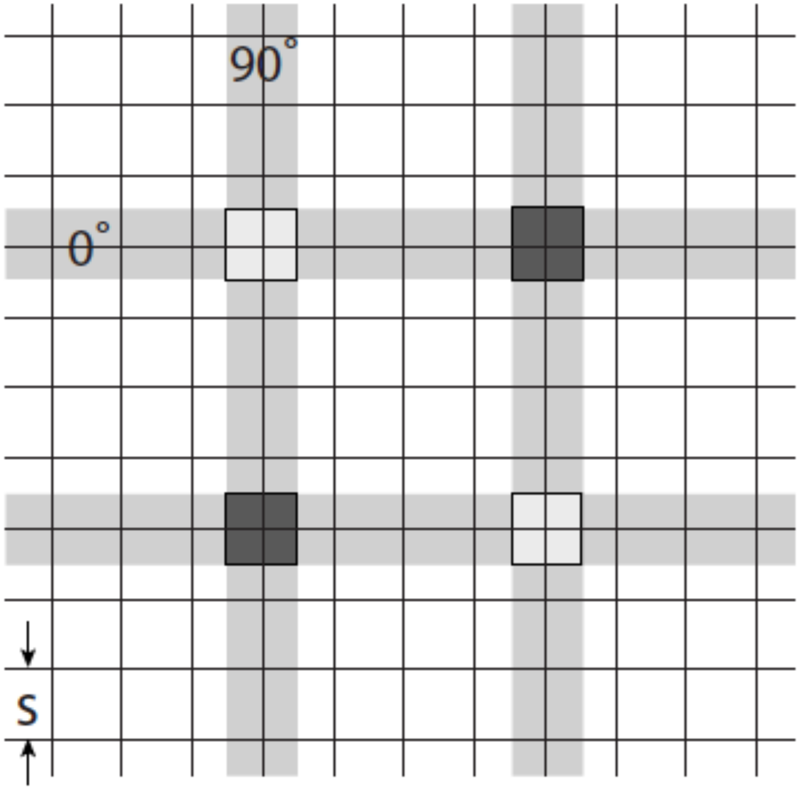

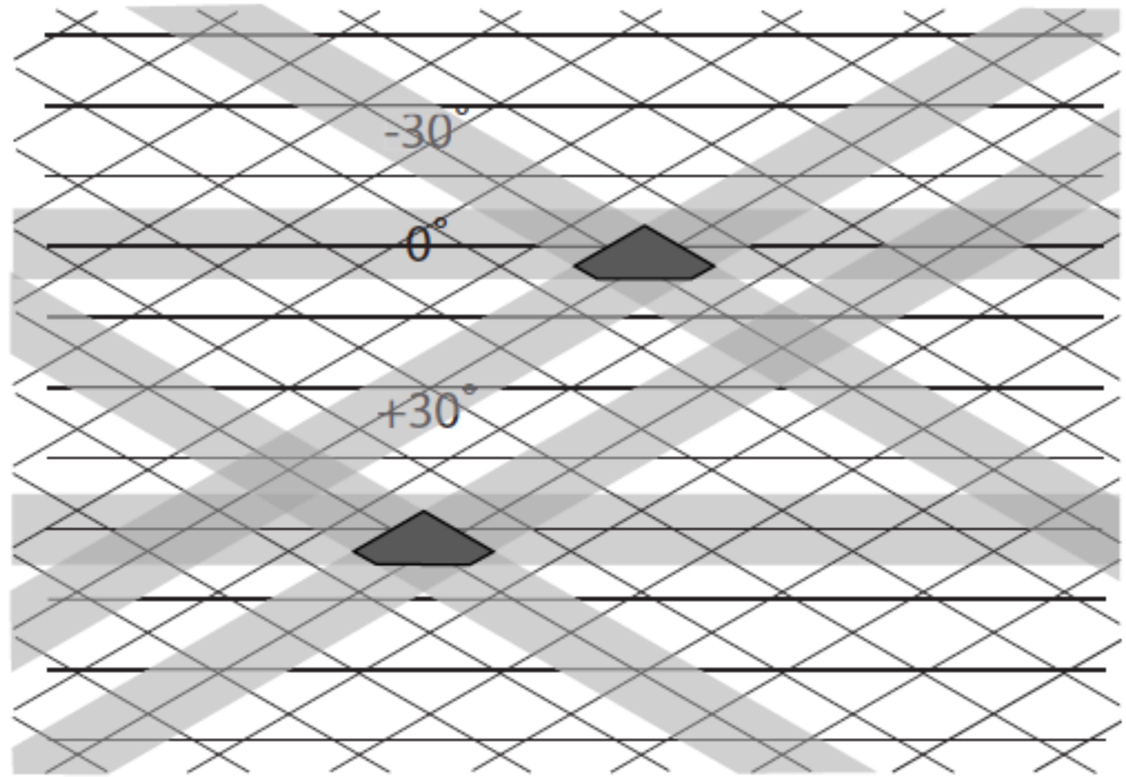

Kolanoski, Wermes 2015

90° "stereo" arrangement
best for resolution
but n^2 "ghost" hits

±30° "stereo" arrangement
(3 layers)
small angles often easier due to wire fixations or R/O
no ghosts in this example

The Driftchamber (usually operated in proportional mode)

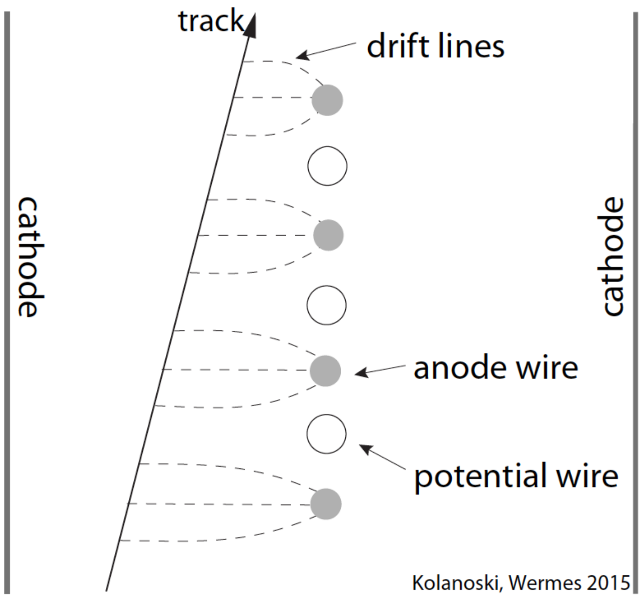

- MWPC limited for very narrow wire spacing due to electro-static repulsion: typ.: s > 1mm for ⃠ 10 μm, l = 25 cm
- better resolution obtained by measurement of arrival time of the electron cloud (measured by TDC or similar)
- need additional "potential wire" to avoid low field regions
- space point to drift-time relation is usually field-strength dependent and thus is non linear (-> calibration)

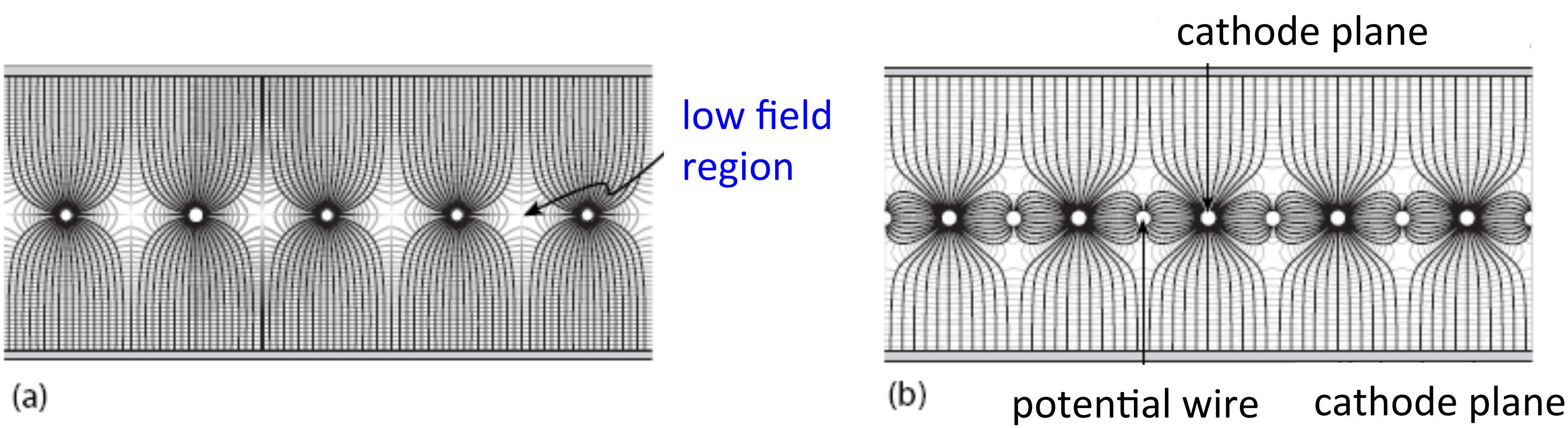

Long drift cells: the Jet Chamber

+ many hits per particle track (~ 135 µm res.)
+ but still only modest number of wires needed in total
+ homogeous E-field → easy space point to drift-time relation

± large drift distances

- get 3D space point by charge division on wire
- multi-hit electronics → good 2-track resolution
- "staggering" of anode wires to resolve the left-right ambiguity

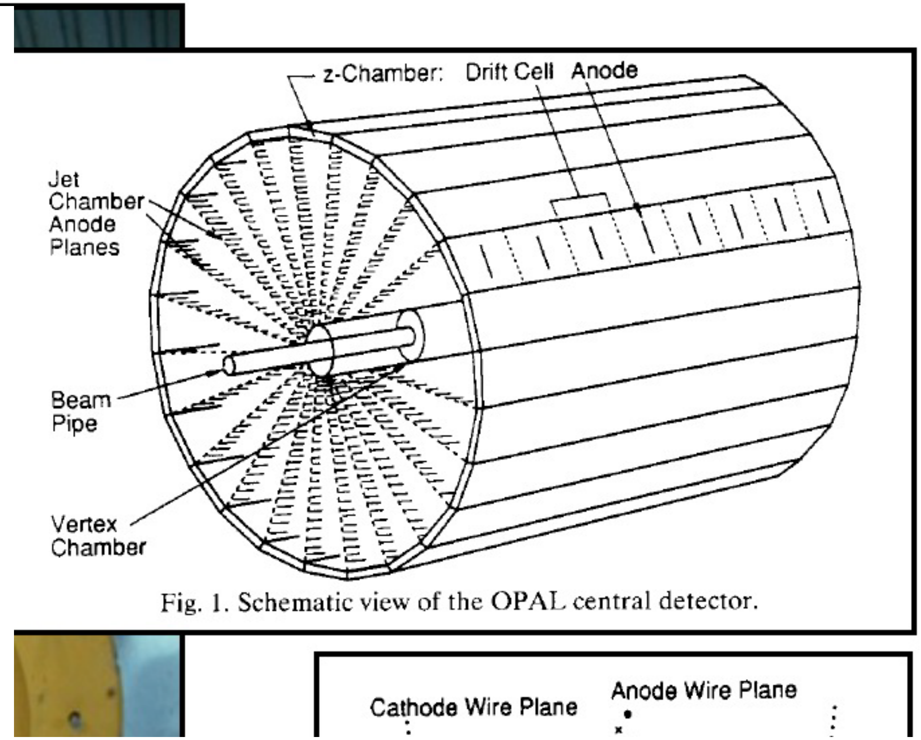

Fig. 1. Schematic view of the OPAL central detector.

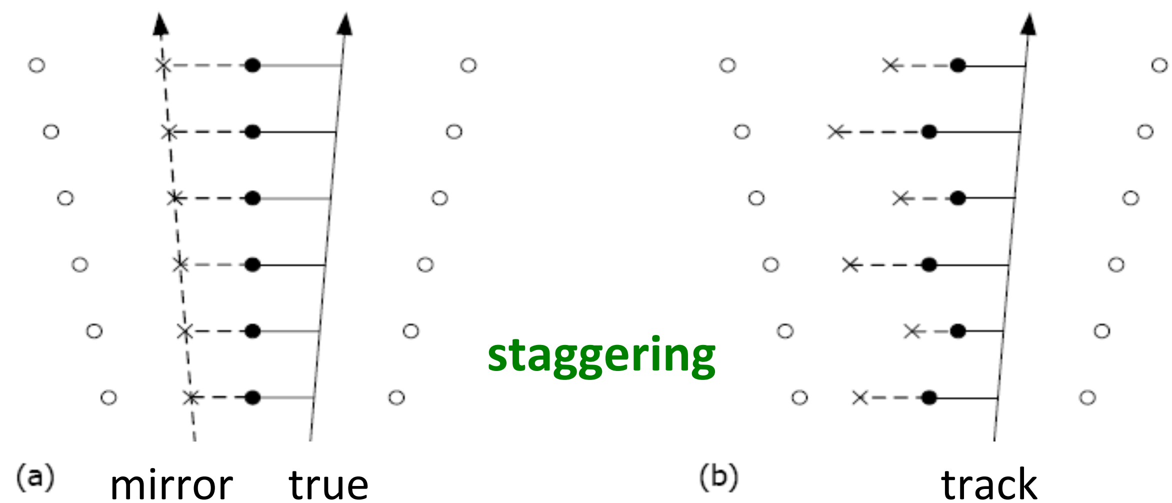

z-coordinate measurement

“stereo” wires in a cylindrical geometry

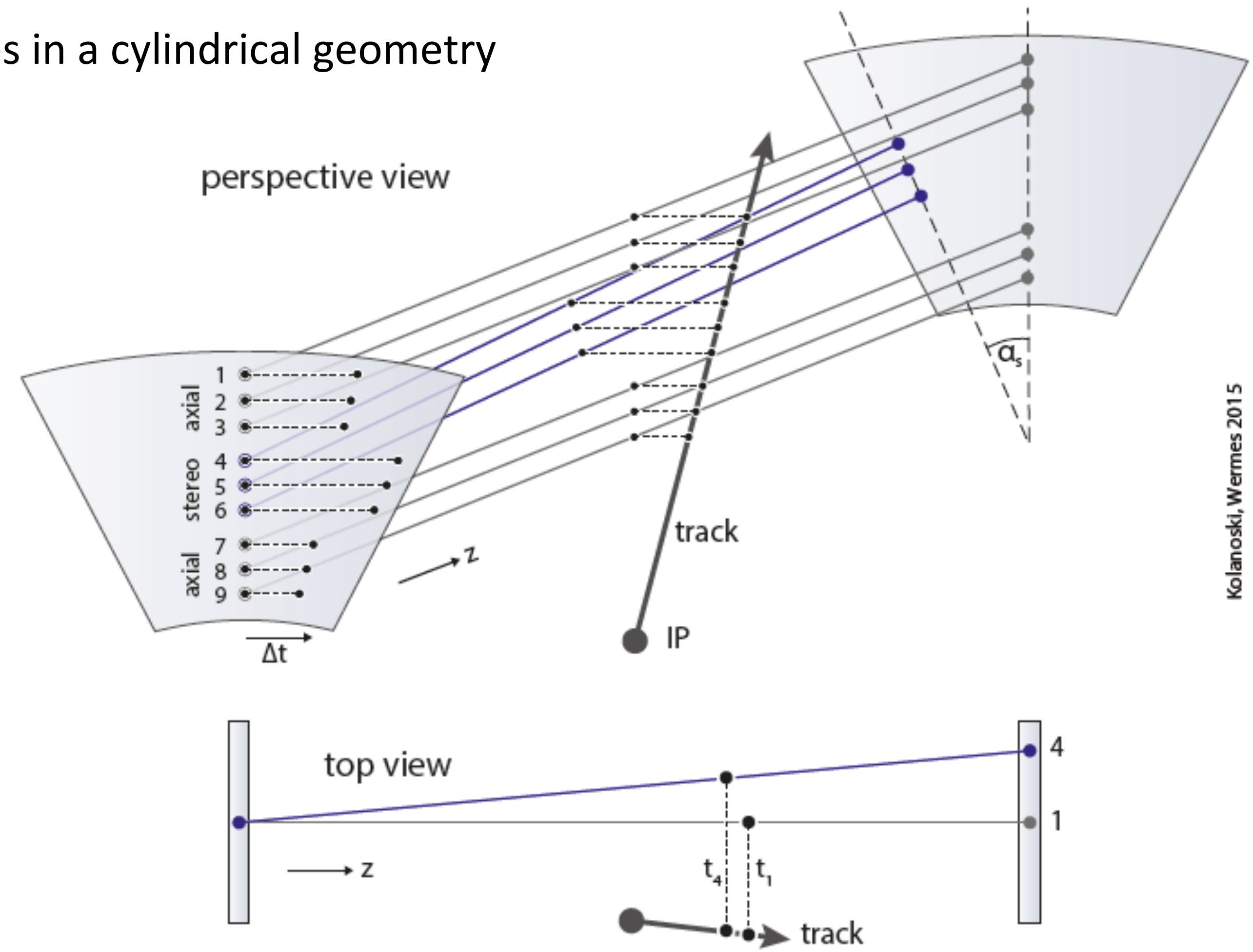

$$\sigma_z = \sigma_{r\phi} \cdot \frac{1}{\sin \alpha_{\text{stereo}}}$$

+ (still) relatively good spatial resolution
- one looses wires for other tasks (rϕ)
- not practical in high track density

Time Projection Chamber

invented by D. Nygren (1976)

universitätbonn

large wire-less volume

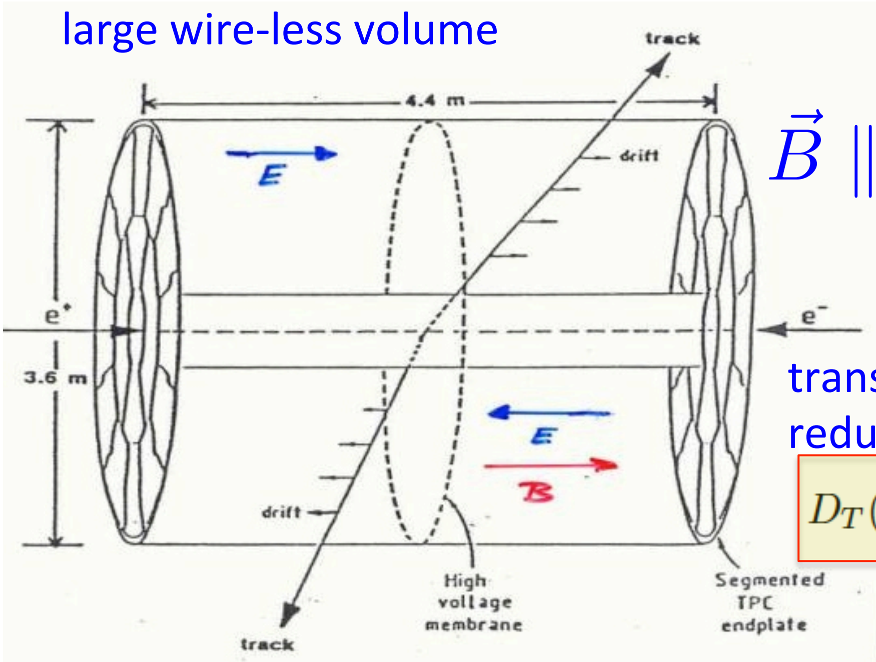

$\vec{B} \parallel \vec{E}$

transverse diffusion reduced

$$D_T(B) = \frac{D_T(0)}{1+\omega^2\tau^2}$$

long drift along , amplification at end of long drift

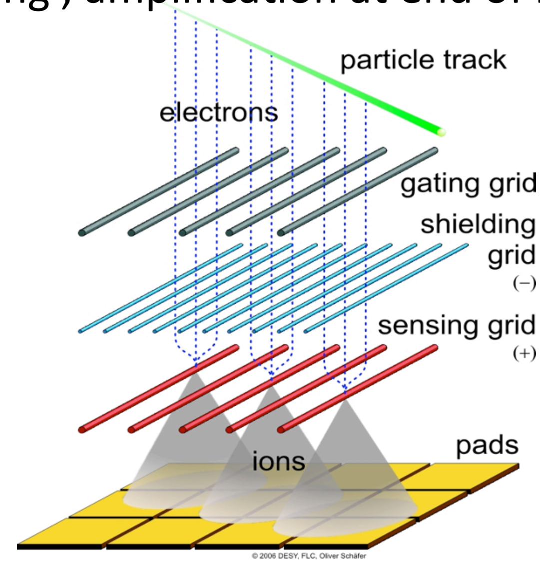

pulsed

prevent ion-feedback by gating grid

- full 3-D reconstruction (voxels): xy from wire/pad geometry at the end flanges; z from drift time
- 3D track information recorded -> good momentum resolution
- also dE/dx measurement easy -> particle ID (not topic of this lecture)
- large field cage necessary
- typical resolutions: in rφ = 150-400 µm   in z ≈ mm
- challenges
  - long drift time -> limited rate capability
  - large volume -> geometrical precision
  - large voltages -> potential discharges

ALICE TPC

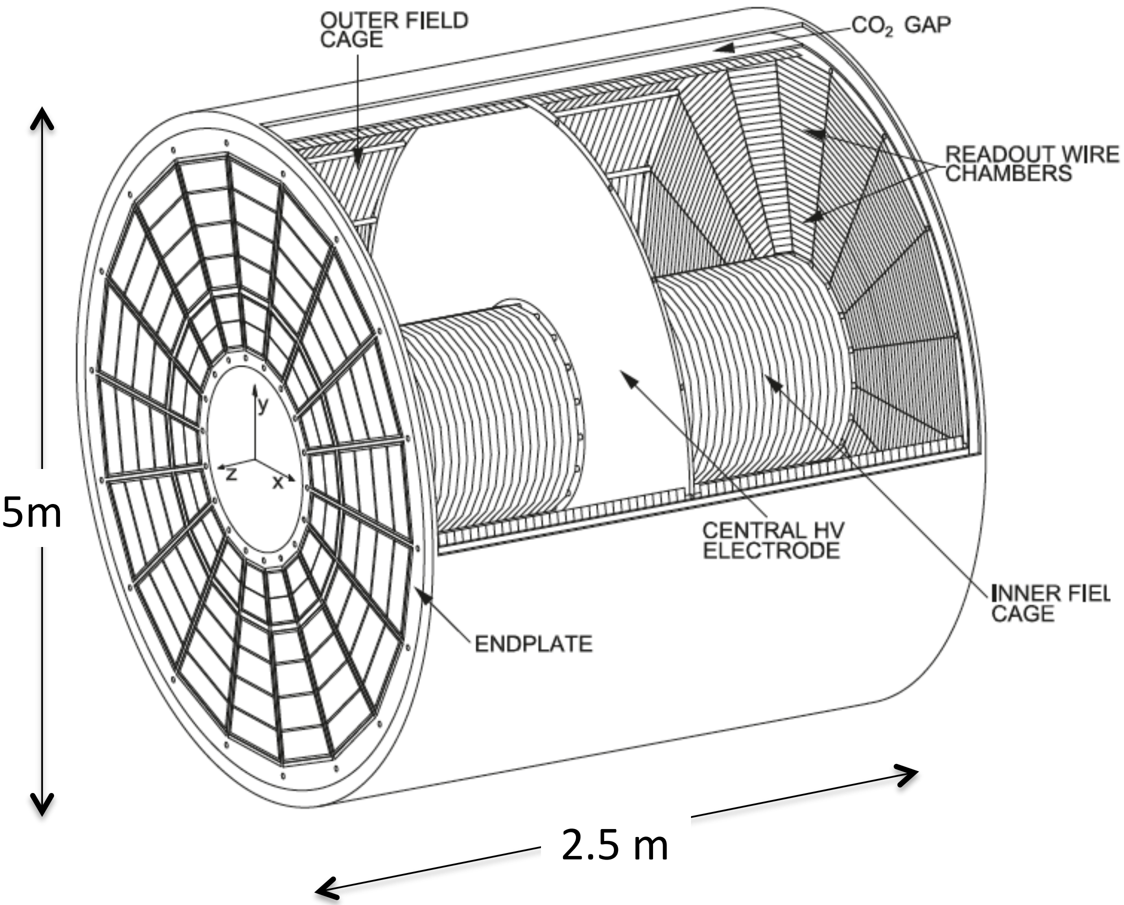

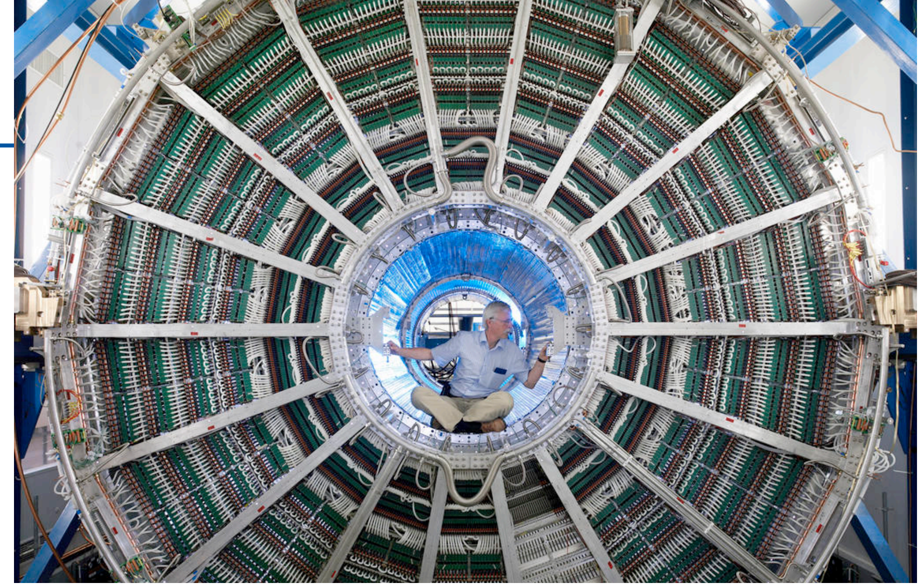

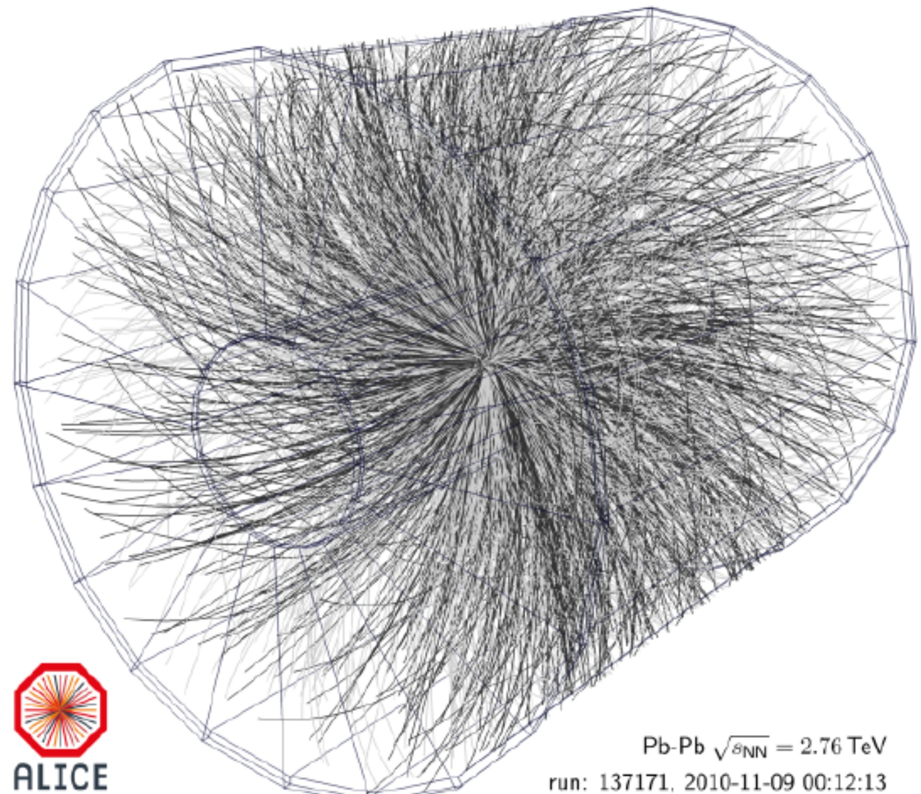

$$\sigma_{x,y,z} \approx 1\,mm^3$$

Big TPCs in experiments

universitätbonn

Parameter/Experiment	PEP4 [612]	ALEPH [100]	ALICE [72]
Volume (m^3)	5	20	26
$\sigma_{r\phi}$ (µm)	130–200	170–450	800–1100
σ_z (µm)	160–260	500–1700	1100–1250
Zweispurtrennung (mm), T/L	20	15	13/30
σ_p/p^2 (GeV^{-1}) (p groß)	0.0065	0.0012	0.022

Developments accomplished in the context of high rate applications (i.e. LHC)

What is different (to before) for LHC pp experiments?

universitätbonn

- particle rates ($\mathcal{L} = 10^{34}\ cm^{-2}\ s^{-1}$) note: heavy ions: $\mathcal{L} = 10^{27}\ cm^{-2}\ s^{-1}$
  - bunch crossing every 25 ns
  - $N_{trk} = \sigma\ \mathcal{L} = 100\ mb \times 10^{34}\ cm^{-2} s^{-1} \times 120 \approx 10^{11}$ tracks/s in 4π
    this is 10^6 times the track rate at LEP
  - @ r = 5cm => 9.5 tracks/cm²/25 ns but only 10^{-4} per pixel (100x100 μm²)
- radiation level (@ r = 5cm, per detector lifetime)
  - ionizing dose = energy/mass (J/kg) = 100 Mrad
  - non ionizing fluence (breaks the lattice) = 10^{15} particles per cm²
  - affects ageing on wires, electronics, …
- way out
  - high granularity, small cells
  - high timing precision << 25 ns
  - solid state detectors (-> lecture 3)
    - micro structuring => highest granularity
    - but: sensitive to radiation (different to gaseous detectors at moderate gas gains)

Straw tubes

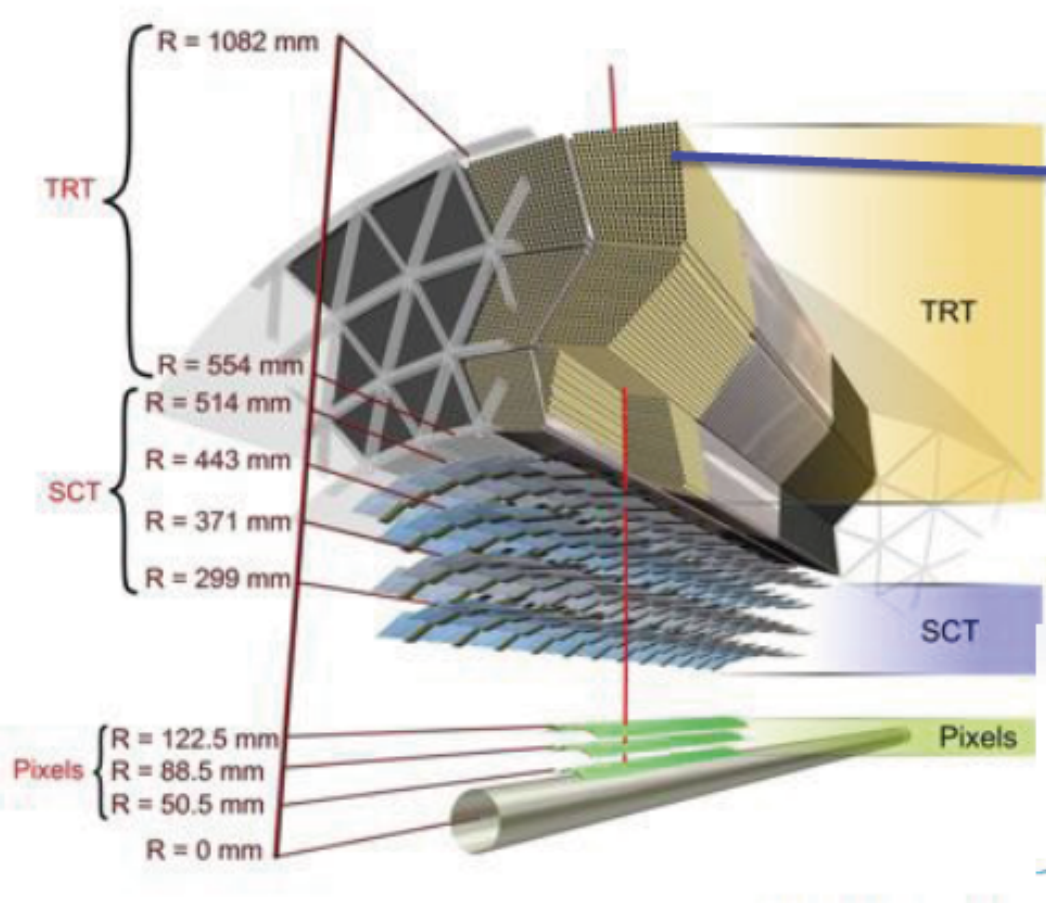

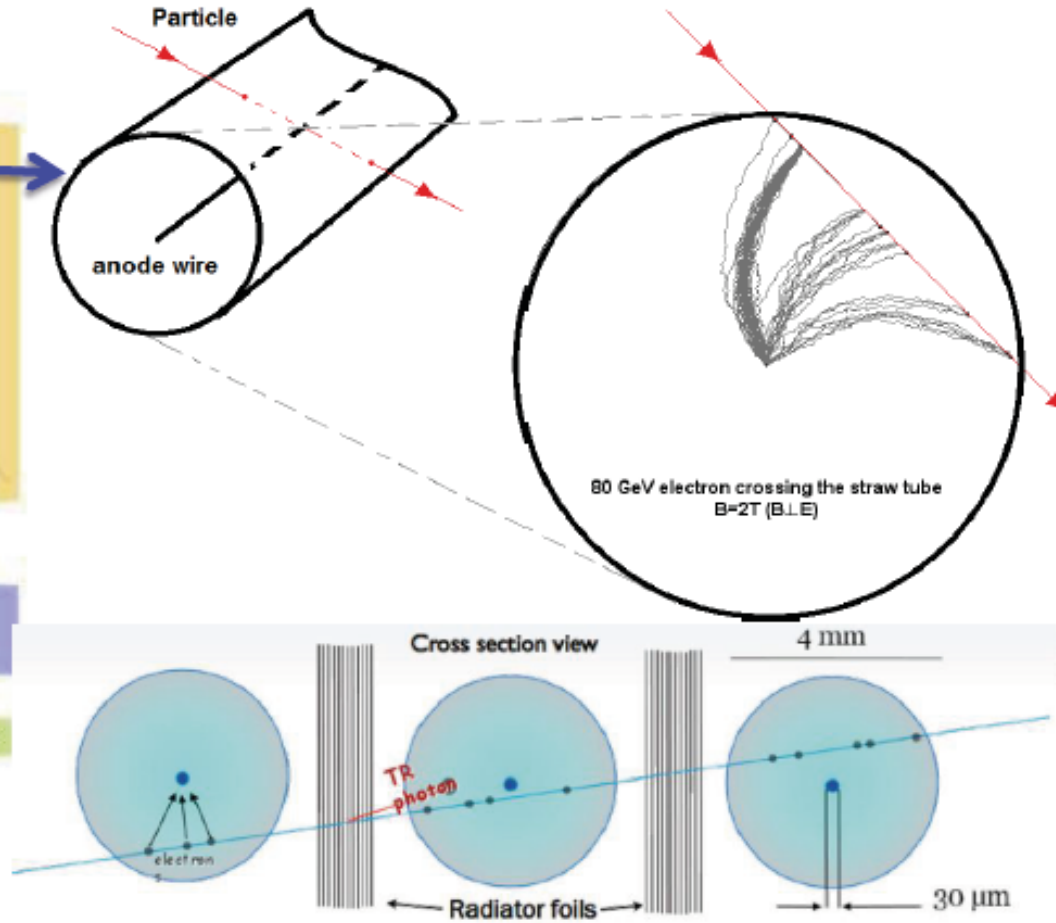

ATLAS ID Barrel

- diameter = 4 mm
- ~36 hits along a barrel track
- gas: Xe - CO_2 - O_2 (70%:27%:3%)
- serves as tracker and e- ID at the same time
- can better cope with high rates due to individual units and short drift distances

MPGCs (Micro Pattern Gas Detectors)

- advances in micro structuring also entered clever chamber designs
- goals:
  - thin gap
  - high rate capability (100 x MWPC)
  - high resolution

GEM (Sauli et al.)

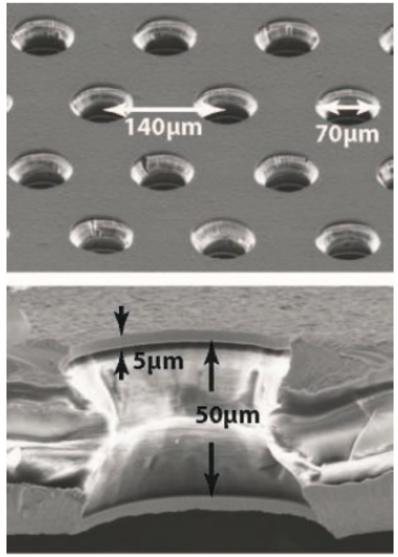

high field regions

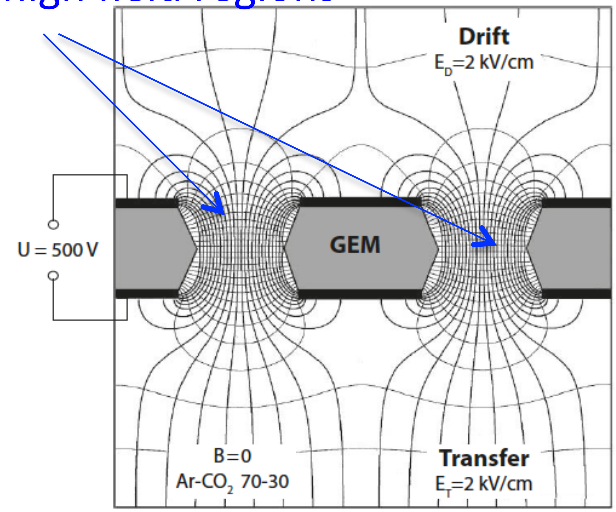

MSGC (Oed et al.)
prone to sparks

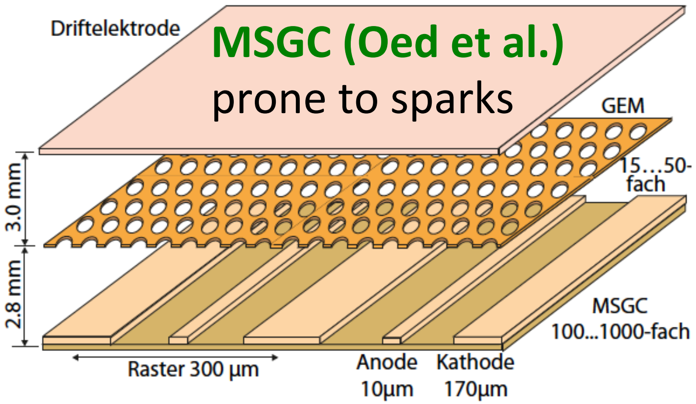

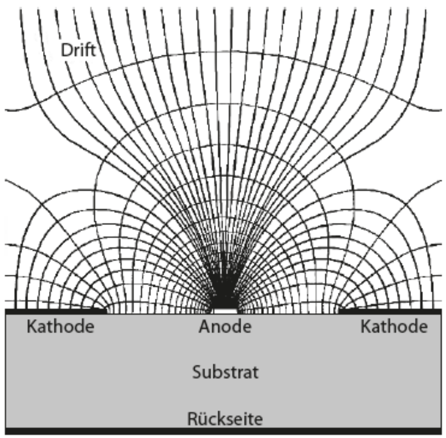

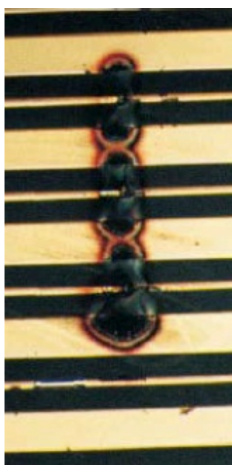

today's standard: Triple GEMs (stand alone detectors)

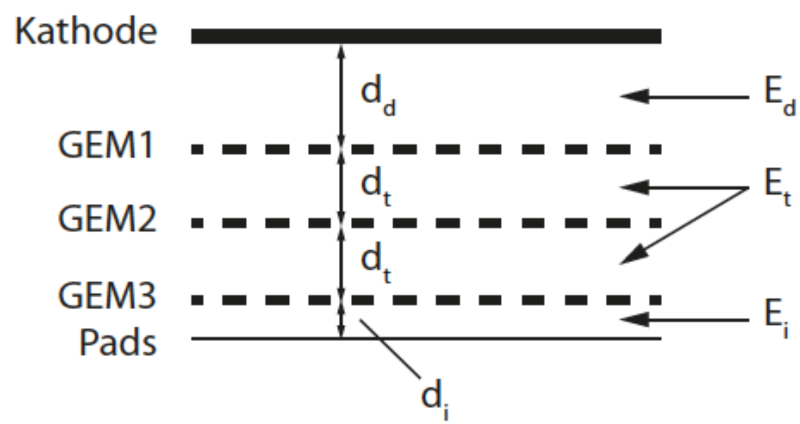

MICROMEGAS (MICRO MEsch GASeous Structure)

universitätbonn

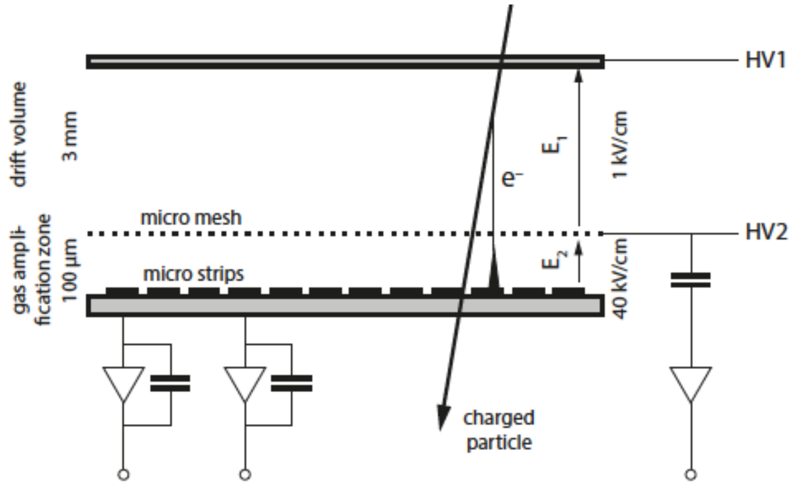

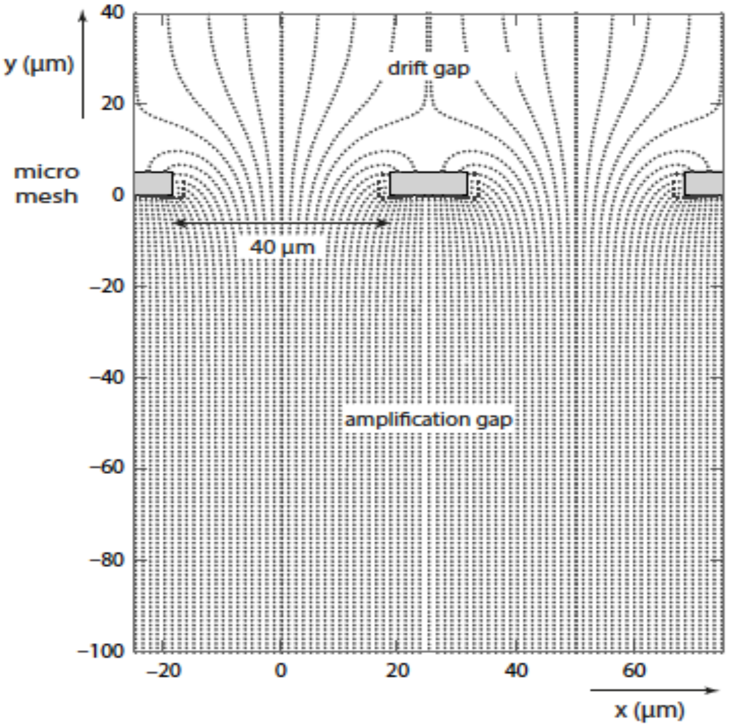

- separation of drift region and (short) amplification region by a micro grid
- R/O of induced charges by patterned electrode
- fast induced signals
- need precise grid alignment
- new development: INGRID structure obtained by "post processing" of grid directly on R/O chip

INGRID structure

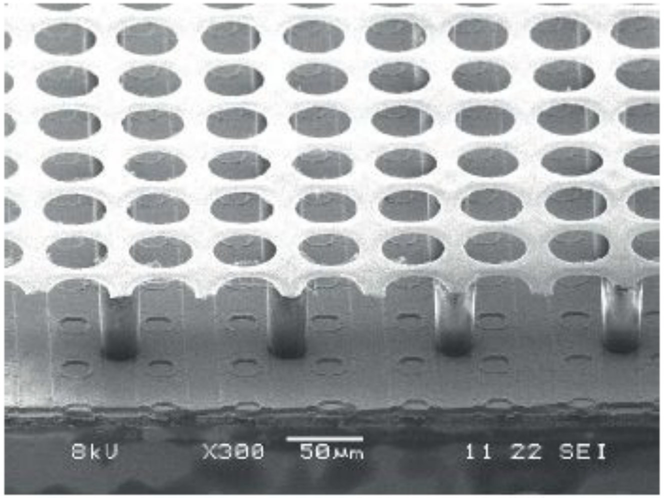

RPCs (resistive plate chambers)

- target **high timing precision** (trigger and timing chambers, e.g. ATLAS Muon Spectrometer)

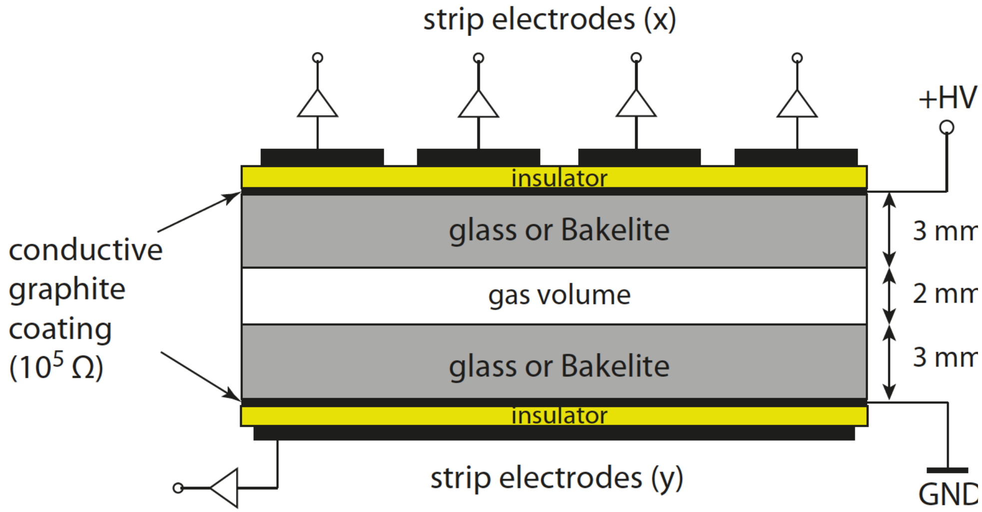

- use high ohmic (10^8-10^{12} Ω cm) plates (glass, Bakelite) with small gap (2mm)
- operation (~10 kV) in avalanche (shorter quench times) or (~100kV/cm) streamer mode (larger and faster signals)
- induced signals reach through to patterned electrodes
- large signals: <100pC streamer, <10pC avalanche
- gas with high ionisation density and high quenching efficiency needed:
  e.g. 94.7% $C_2H_2F_4$, 5% i – C_4H_{10}, 0.3% SF_6

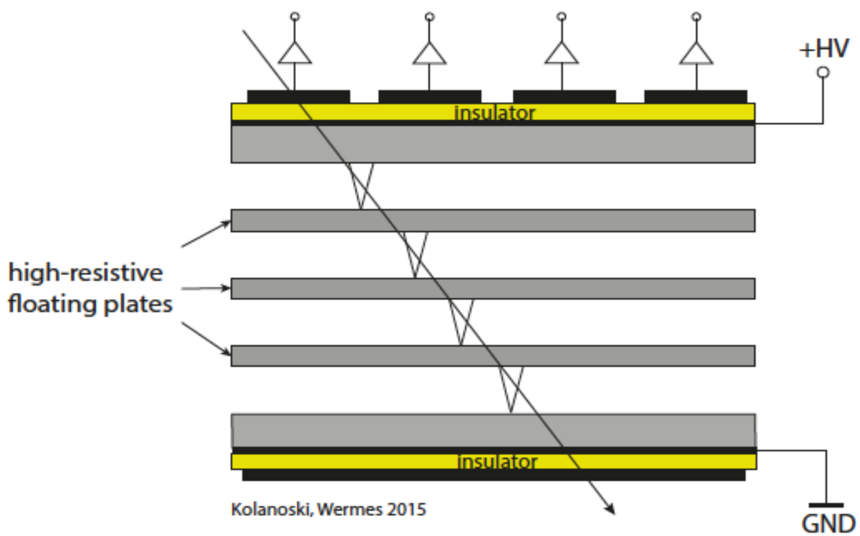

Kolanoski, Wermes 2015

Trigger-RPC avalanche mode		Timing-RPC streamer mode	
E =50 kV/cm		E =100 kV/cm	
α =13.3/mm	η = 3.5/mm	α =123/mm	η = 10.5/mm
v_D=140 μm/ns	d = 2 mm	v_D=210 μm/ns	d = 0.3 mm
σ_t =1 ns		σ_t =50 ps	
ϵ =98%		ϵ =75%	

End of Lecture 1